SHORT TERM GRANT REPORT

ON

EXPERIMENTAL INVESTIGATION AND NUMERICAL METHOD OF THERMAL CONTACT RESISTANCE FOR HARD AND SOFT MATERIALS

BY

MOHD ZULKIFLY ABDULLAH
ZAINAL ALIMUDDIN ZAINAL ALAUDDIN
K. N. SEETHARAMU
MOHD YUSOFF IDROAS

SCHOOL OF MECHANICAL ENGINEERING
ENGINEERING CAMPUS
UNIVERSITI SAINS MALAYSIA

ACKNOWLEDGEMENT

The authors express thier gratitude to **Encik Mohd Kamal Ismail, Encik Najhan Awang, Fabiam William and Hafizul** for their contributions in this project.

The author would like to thanks **the Universiti Sains Malaysia and Ministry of Science, Technology and Innovation** for their financial supports for this project.

At last but not least, a special thanks to the **School of Mechanical Engineering** for their supports and providing a space for the experimental set-up.

Mohd Zulkifly Abdullah (Project Leader)
Zainal Alimuddin Zainal Alauddin
K. N. Seetharamu
Mohd Yusoff Idroas

EXPERIMENTAL AND NUMERICAL METHODS ON THERMAL CONTACT RESISTANCE FOR HARD AND SOFT MATING MATERTIALS

ABSTRACT

Literature studies have shown that the thermal contact resistance is among the problems in thermal management for microelectronic devices. The interfaces surface roughness is one of the factors contributed to the thermal contact resistance. Therefore, an experimental investigation has been made in order to identify the parameters contributed to the thermal contact resistance in general. The experiments conducted in a rig mounted with measuring instrument and tested in ambient and vacuum condition (-75kPa). The experimental rig consists of brass load shaft, vacuum pump, cooling system, data acquisition, thermocouples, PC, heaters and voltage regulator. The test has been made on the specimen with smooth surfaces (<1.0μm) and rough surfaces (>1.0μm) for brass, aluminum, stainless steel and mild steel respectively. Contact pressure is varied up to 132kPa during the experiment. For the entire specimen, the smoother their surface roughness and the lower hardness of the material provided better thermal contact than other material as shown from the results. The results in vacuum condition are better than in ambient condition. In this study, the thermal contact resistance in Li-ion cell battery also has been made where the results obtained showed similar trend with previous research work. Cathode has the highest value of thermal resistance followed by anode and separator. The experimental results obtained are compared with the theoretical prediction. The thermal contact resistance also reduced significantly by increasing the contact pressure in the experiment.

TABLE OF CONTENTS

		Page
ACKNOWLEDGEMENTS		
TABLE OF CONTENTS		
ABSTRACT		
CHAPTER ONE: INTRODUCTION		
1.0	The Fundamental of Thermal Contact Resistance.	1
1.1	Background and Trends.	2
	1.1.1 The importance of studying thermal contact resistance.	3
1.2	Objectives	4
	1.2.1 Scope of Works	5
CHAPTER TWO: LITERATURE SURVEY		
2.0	Introduction	6
2.1	The important of the thermal contact resistance and the Effect of the thermal and mechanical parameters.	7
	2.1.1 Thermal contact resistance at mechanical joints.	8
2.2	Numerical simulation on thermal contact resistance.	11
	2.2.1 Thermal Contact Resistance Model and Theoretical Prediction.	11
	2.2.2 Thermal Constriction and Spreading resistance (conductance) models.	14
	2.2.3 The Finite Element Method in Thermal Contact Resistance.	16
2.3	Previous experimental works and the method of applying contact pressure.	18
	2.3.1 Observation on the mechanical and surrounding factors in experimental method.	20
	2.3.2 Steady state condition in thermal contact resistance.	23
	2.3.3 Coated layer, Thermal interface materials (TIM)	16

And Phase change materials.
2.3.4 Thermal contact resistance test on different materials and purposes 18
CHAPTER THREE: THEORETICAL PREDICTION
3.0 Introduction 33
3.1 Gaussian distribution of the asperity height and slopes 33
3.2 Plastic Contact Resistance Model of Cooper, Mikic and Yovanovich. 35
3.2.1 The estimated real contact area from CMY model 38
3.3 Elastic Contact Resistance Model of Mikic and Greenwood and Williamson. 38
CHAPTER FOUR: EXPERIMENTAL LAYOUT
4.0 Introduction 40
4.1 Development of test rig apparatus 41
4.1.1 The important parts of the experimental rig 42
4.1.2 Thermal and cooling system 44
4.1.3 Specimens preparation 45
4.2 Experimental set up and testing procedures 48
4.2.1 Test procedure for Li-ion cell battery layers (dry test) 50
4.3 Data and uncertainty measurement of the experimental results 51
CHAPTER FIVE: RESULT AND DISCUSSION
5.0 Experimental result overview 54
5.1 Effect of surface roughness to the temperature drop between Contacting surfaces 55
5.1.1 Effect of smooth surface to the temperature drop at the interfaces 56
5.1.2 Effect of rough surface to the temperature drop at the interfaces 63
5.2 Effect of the contact pressure to the thermal contact resistance 70
5.3 Effect of the material hardness on the thermal contact resistance 71
5.4 Results Comparison and Discussion 75
5.4.1 Comparison between ambient and vacuum conditions 76
5.4.2 Comparison between experimental and prediction 79
5.5 Thermal contact resistance in Li-ion cell battery 82
CHAPTER SIX: CONCLUSION
6.0 Conclusion 86
6.1 Future works 87
References 88

CHAPTER ONE

INTRODUCTION

1.0 The Fundamental of Thermal Contact Resistance

Thermal contact resistance is a part of the heat resistance that often effecting the thermal system especially the system involving the compact and complex components. The effects are clearly observed in the component that needs an optimum heat transfer rate. Whenever heat flow at the interface of two materials in contact must be controlled or estimated especially the temperature drop at the interface through experiment or prediction. The thermal contact resistance can be defined as the ratio of the temperature drop to the heat flow across two parts or interface and can be described as shown in Figure 1.

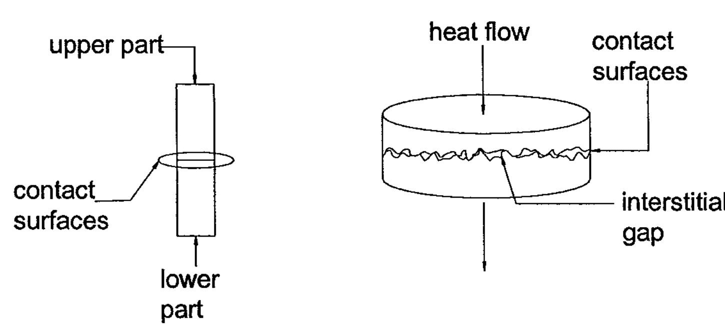

Figure 1.0 Thermal contact resistance between two mating surfaces.

There are two assumptions contribute to the heat conduction between interfaces. The first principle is that the heat flux will start from solid point to another solid point because of proper contact and another principle is that the heat conduction will occur through fluid medium such as air that trapped in the interstitial gap because of improper contact. The air or gases trapped in the interstitial gap increase the thermal contact resistance due to the small value of air thermal conductivity comparing to other materials.

1.1 Background and Trends

The growth in technology such as modern internal combustion engine, biomedical prosthetics, aerospace, semiconductor industry with the increase of microprocessor capability together by reducing of it size lead to the interesting of this topic to be studied. For example, nanotechnology is going to be developed to replace with micro technology that has been used in last century. Hence, the thermal management for such technology also has to be improved which including the thermal contact resistance. However, most of practical contact surface were rough because to produce smooth surface is more difficult where proper machining technique must be used. An electronic part such as silicon chip encapsulation is made by plastic mold material with rough surfaces. The heat sink surface acted as a heat removal or heat spreader, usually bonded to the chip surface to absorb heat also has rough surface approximately above 1μm. Thus, the thermal contact conductance between these surfaces will be very low and it will influence the overall thermal management in the system. Thermal interface material (TIM) such as thermal grease and copper foil are widely used nowadays to overcome the high thermal contact resistance value by estimating their capabilities to improve contact between two surfaces (Gwinn and Webb, 2003). By coating the contact surface with high thermal conductivity material such as silver, copper or metallic coating is also used nowadays to improve the thermal contact.

1.1.1 The importance of studying thermal contact resistance

In many systems, thermal management always needs to be considered. The value of thermal contact resistance most of the time must be reduced or in different way has to be increased to suit the thermal systems requirement for example to insulate the spacecraft or satellite from hot surrounding in outer space. The selection of material to use based on their thermal contact resistance value is still unpredictable by using any theories that suitable for all cases. Many parameters must be taken into account to get the almost exact value. Besides, it depends on the material property and surrounding condition. By using unsuitable material as a heat conductor or spreader and without good surface finishing between interfaces will cause improper contact. The thermal interface material (TIM) that is commonly used in electronic industries involves limited contact area between chip and microprocessor with the heat sink. For large nominal contact area, applying (TIM) will no longer reasonable because it is costly. Coating technique is suitable for large contact area but the factor of cost and the low efficiency comparing with (TIM) again has to be considered. For all these reasons, the study of thermal contact resistance is still necessary where the contact between two interfaces could be improved by predicting the thermal behavior of the material itself without applying (TIM) or coating technique. Moreover, before applying (TIM) or coating the surface contact, the value of contact thermal resistance must be predicted first in order to select the best solution.

1.2 Objectives

The objectives of this research are as mentioned below;

- To design and built proper experimental rig by considering the surrounding of the test section. The rig had been fabricated where the experiment provided ambient and vacuum environment around the test section.
- To make comparison between two set of data that has been done in different environment.
- To investigate the effect of surfaces roughness of the test specimens during thermal contact where the surfaces has been ground and polished to provide different type of surface which is smooth and rough.
- To investigate the effect of material hardness in thermal contact resistance for different types of hard and soft mating materials.
- To investigate the effect of contact pressures on thermal contact resistance value during the experiment.
- To obtain the thermal contact resistance value for Li-ion electrode stack and compare with the previous results.
- To estimate the value of thermal contact resistance using a numerical method by considering the important parameters such as hardness and surface roughness of the specimens.
- To compare the experimental results with theoretical results.

1.2.1 Scope of Works

The experimental test considered on four different types of hard mating material with smooth and rough surface. Rough surface is the roughness value above 1μm while smooth surface is below that value. The test rig is developed for both different environments and pressure. The specimen has been insulated to reduce convection in ambient test environment. A test also has been done on Li-ion mobile cell battery. The results obtained have been compared with previous experimental work. The surfaces roughness of the materials is used to obtain the thermal contact resistance by theoretical calculation. This research concentrated on the experimental works to identify the important parameters that provide significant effects on thermal contact resistance. Numerical calculation to predict the thermal contact resistance also has been made.

CHAPTER TWO

LITERATURE SURVEY

2.0 Introduction

Thermal contact resistance has been studied through experimental test and theoretical prediction. In this chapter, some of the previous works have been discussed. In thermal conduction problem, the temperature drop between interfaces always been neglected as mentioned by Incropera and DeWitt (2002). However, the optimization of thermal management on many systems nowadays must concern on the existence of thermal contact resistance. Many experimental works and numerical prediction has been developed to achieve the goal of finding the best solution. Wolf and Schneider, (1998) in their surveys found that conduction between interfaces has been discussed since 1943 with first one-dimensional model considered on parallel heat flow through the asperities and the interfacial material.

In the first part of this literature, the important parameters of the thermal contact resistance and the case examples have been reviewed. Factors affecting the thermal contact resistance also have been stressed in many literatures. These factors have been observed from the results obtained through various experimental investigations. The methods of experimental and theoretical prediction together with the development of the thermal contact resistance model became the next topic to be discussed. Some conclusion revealed at the end of this chapter to support the experimental works that has been done in this study.

2.1 The important of the thermal contact resistance and the effect of the thermal and mechanical parameters.

According to Wing Aung (1991), the description on the real contact, the important geometric, thermal and mechanical parameters must be considered. The geometry of contacting surfaces referred to the surface roughness, asperity slope and waviness. While for thermal parameters referred to the conductivity of both solid to solid contact and the interstitial fluid. Mechanical parameters then referred to the hardness and flow pressure of the contacting asperities which caused the plastic deformation of the highest peak of softer substrate.

As mentioned before by Wing Aung (1991), the real contact area is probably too small compared with the nominal contact area. The same idea has been proposed earlier by Greenwood and Tripp (1970) that real contact area is extremely small. They also concluded that almost all surface contact models considered the surface roughness just at one surfaces while another surface is assumed to be flat. They had studied on the model of contact surfaces which considered on both surface roughness and finally came out with the statement that any model of contact between surfaces with both surfaces assumed to be rough can be model in which only one surface is rough.

Yeau-Ren Jeng et al. (2004) introduced the theoretical model based on surface contact area. They considered on the mechanical parameters which caused elastic, elastoplastic and fully plastic deformation. The asperity deformation can be described first by using the interference factor to recognize the deformation level. If the interference factor is very small, the asperity deforms elactically. For plastic deformation, the interference factor must be at least 54 times larger than the interference factor at initial yielding. For elastoplastic deformation, the value of interference factor must be between the factor at initial yielding and the factor for fully plastic. Then, by combining the statistical surface asperity distribution for two contact surfaces, the real contact area for elastoplastic deformation can be found. Finally, all the mechanical parameters such as elastic, plastic and elastoplastic deformation are combined to get the total real contact area between surfaces.

Flatness deviation and surface waviness of any surface in contact is said to be the macrocontact parameter while surface roughness or surface topography obtained by surface profilometer from the surfaces in contact is called microcontact parameter. Yeau-Ren Jeng et al. (2004) again stressed that the fundamental of thermal contact resistance is based on the real contact area. For this reason, all the mechanical properties which affect the contact area such as the macrohardness and microhardness are important. The surface microhardness can be obtained from the material hardness or macrohardness. It is used to get the pressure that caused the deformation of the asperities and to calculate the real contact area between interfaces. Several types of unit can be used to represent the value of hardness for example the often used units such as Vickers, Rockwell and Brinell. Meyer hardness has been used in the model proposed by Wolf and Schneider (1998). The model used the microhardness value which converted from the macrohardness value.

2.1.1 Thermal contact resistance at mechanical joints.

Wing Aung (1991), clearly mentioned about the general parameters influenced the thermal conductance between contact spots, gap and joint. When the interstitial fluid or gases substitute with vacuum surrounding, the heat flux will converge and diverge at the microscopic contacting surfaces. Usually, the temperature drop at the interface is measured by extrapolating the temperature value of one dimensional temperature distribution between two contacting bodies in steady state condition. The real contact happened just between microscopic peaks and valleys exist on the surfaces. Thus, the real contact between interfaces can be described as follows;

- Intimate contact exactly occurred in micro contact of the interface with the contact ratio between real contact and nominal surface contact is less than 2%.
- The real contact pressure referred to the contacting peaks of asperities. The surface can be measured by interface thickness which is range between 0.5μm for smooth surface and 60μm for very rough surface.
- Third substances can be air, liquid and other interface materials.
- The heat transfer between interfaces finally can be described by three modes which are conduction through real contact area, conduction through interstitial fluid or gases and by radiation if test in vacuum.

Madhusudana (1999) has studied on thermal conductance of cylindrical joints. This cylindrical joint can be found for many examples such as in the heat exchangers, plug and ring assemblies and shrink-fit cylinders. Common theoretical model investigated flat mechanical joint where few of literature concentrated on cylindrical joint. His effort enabled us to predict the thermal behavior such as thermal contact resistance at the interfaces. For flat joint, heat transfer can be controlled by varying the surface roughness and waviness together by increasing the contact pressure. Many thermal models for surface contact between flat joint has been discussed as the effecting parameters mainly have been recognized.

For cylindrical joint, Madhusudana (1999) has pointed out some different parameters that must be considered such as the material thermal expansion. For his prediction, inner and outer of joint material has been varied. Aluminum and stainless steel with high and low thermal expansion are tested. The bond resistance also can be predicted through his investigation where both bond resistances between inner and outer material can be used to describe the thermal contact conductance at the cylindrical interfaces. His study has been compared with a few experimental results where good agreement has been found. However, only a few experimental tests were available recently so that more experimental works need to be done for cylindrical contact in the future. The theory predicted that for better contact, the inner material act as a heat source must possess high thermal expansion value so that the outer material will have a good bonding at the interfaces together with a good thermal contact conductance at high temperature condition. The result showed that for aluminum-stainless cylindrical contact combination has the highest contact pressures at the interfaces while for the same material, aluminum-aluminum or stainless steel-stainless steel showed smaller contact pressure and the stainless steel-aluminum combination showed the lowest. In overall, the temperature gradient, the material used and the material orientation in cylindrical contact will affect the contact pressure at the interfaces. The interface surface roughness and other parameters considered for flat joint also has to be considered for cylindrical joint.

2.2 Numerical simulation on thermal contact resistance.

There are many form of an equation involving thermal conduction can be derived from Fourier's Law. The basic law is one-dimensional Fourier's law of heat conduction which concentrated on the thermal behavior. The measurement of temperature at certain distance between two portions can be made by extrapolating the temperature distribution between the two portions in one-dimensional axis. This method has been applied in many analytical and experimental investigations on thermal contact resistance.

2.2.1 Thermal Contact Resistance Model and Theoretical Prediction

Wolf and Schneider (1998) used Veziroglu theory, where the thermal contact resistance is predicted by using a few important parameters which are an effective gap thickness, the conductivity of interstitial fluid or gas trapped between the interfaces, conductance number obtained from the graph and finally the nominal contact area. While the theoretical development with experimental verification of the thermo-mechanical model have been made by Antonetti & Yovanovich which considered for coated and uncoated contact conductance (Wing Aung, 1991). For Veziroglu and Antonetti & Yovanovich theories, both considered on the surface roughness and hardness of the materials.

Salti and Laraqi (1999) developed three-dimensional numerical model using finite volume method in order to study the thermal behavior between two sliding bodies. The values of temperature and thermal contact resistance have been derived from their model during sliding. The model has been described as a two sliding bodies, where the first body is rough, stationary and comprises numerous square-shaped asperities distributed over the contact plane. While another body is smooth, moving at a velocity V. The interstitial gap is neglected. Heat transfer is three-dimensional and at steady state. The constriction resistance is the ratio of the difference between average temperatures of the real (A_r) and apparent (A_a) contact areas and the flux. In conclusion, the values of relative contact size, ϵ and dimensionless velocity, V^* must be determined to predict the thermal contact resistance. As ϵ and V^* increase, the thermal contact resistance decreases. Using the same value for two-dimensional model, the value will be two to four times lower than three-dimensional model.

Kraus and Bar-Cohen (1983) simplified the model for thermal contact resistance into two solid metal bars that brought into intimate contact. The apparent contact area composed of metal to metal contact, A_c and void area, A_V. They proposed a better theory to determine the proper value of A_c, A_V and surface height or roughness, δ_V. They clearly mentioned on the geometry of contacting surfaces which involved surface slope asperities, the surface waviness and nominally flatness surfaces. The factors influenced the thermal contact resistance also being discussed which included the most important surface roughness parameter. Different models assumed to be used in vacuum condition have been derived with different surface geometry such as the contact between smooth and wavy surfaces, nominally flat and rough surfaces and rough and wavy surfaces. The effect of interstitial fluids also has been correlated with contact spot.

A new method to predict the contact spot distribution has been made by Zhang et al. (2003). The method introduced a new system that used an equiperipheral grid in cylindrical coordinates to see the contact spot distribution for a random number surface roughness model. The surface roughness parameter has been expressed in random numbers model. This model has a close agreement with Gaussian height distribution of surfaces. Computational calculation has been carried out for simulation of three dimensional rough surface model (20mm x 20mm) square plates. The simulation continued with heat conduction simulation based on previous calculation. It is said that beside the advantages of simulating contact surfaces through random number, this new method also presented good numerical prediction result compared to other numerical methods.

Knyazeva (2000) introduced one-dimensional mathematical formulation of the conjugate coupling problem of the thermal elasticity theory with non-ideal contact between substances. The problem is said to be practical interest. A few non-dimensional expressions used to improve the experimental data and the conjugate mechanical problems. It also can be used to debug computational numerical method done by computer. Zhang et al. (2003), presented models as a solution for the problem occurred between metallic cylinders indenting an elastic layer with certain thickness. Both are rigid and assumed to be frictionless. As metal to metal contact always been considered, the contact between metal to elastic layer also has to be considered for many practical use. The machined metal surface obtained from turning process has been model. The elastic layer usually polymers is used based on their special mechanical and thermal properties such as thermal expanding. They concluded that the mechanical model can predict the cylinder contact half-width under varying layer mechanical properties, dimensions and applied load.

Laraqi and Bairi (2002) have suggested on the theory of randomly sized and located contacts for thermal contact resistance. Linear superposition method is used to determine a solution of the randomly thermal macro and micro constriction that related to the macro and micro contact. It is said that the model used showed good agreement with other models with regular contact. Their model is made by using multiple disks with different radius. To produce random contact geometry, the function of relative contact size, the contact disorder, the number of contacts and the radius ratio has been studied. This theory is said to be easy to use and consider numerous contacts.

2.2.2 Thermal Constriction and Spreading resistance (conductance) models.

Anthony et al. (2004) has described the heat flow through the interfaces into a semi-infinite cylinder constriction resistance model. Usually, the gas that trapped between the interfaces has a low thermal conductivity value. As a result, the heat flow is constrained to flow through the contact spots which will cause the constriction resistance. The contact resistance is said to be the combined effect of the constriction resistance at all of the contact spots between two surfaces. The contact spots which spread between nominal contact areas is measured in radius. The constriction resistance modeled by a number of heat-flux cylinders where contact spots occurred at the end of the cylinders surfaces. The final model combined all the contact spots to be semi-infinite cylinder constriction resistance model in two dimensional with symmetric axis. The ratio of constriction to nominal contact radius is used and the contact angle is varied approximately from appropriate ranges based on surface topography data from metal surfaces which has been ground and blasted to get the centerline average surface roughness in the range of 1 to 15 μm. The material thermal conductivity value for silver and stainless steel are used and the air thermal conductivity is assumed to fill the gap.

Alain Degiovanni et al.(2003), has concentrated more on the thermal constriction resistance. The thermal constriction may occur in many levels which in multi-constrictions contact. A simple model has been developed to describe the thermal constriction contact and clearly explained by resistive diagram in their work. Three resistances simplified model has been introduced which included thermal resistance of asperities, thermal constriction resistance at contact spot and thermal resistance of fluid filled in the interstitial gap. The method used to solve the problem for double constriction is firstly considered and extended to multi-constriction model. In this model, micro and macro constriction is considered where microscopic parameter referred to the surface roughness and macroscopic parameters referred to the flatness. The present of interstitial fluid significantly affected the value of overall thermal contact resistance. It depends on the capability of the fluid that may affect the micro-constriction resistance. However, if the present of interstitial fluid is neglected, the value of total thermal contact resistance for double constriction will be more then three times higher then the value of thermal contact resistance that only considered on macro-constriction parameters.

Muzychka et al.(1999) encountered the solution for thermal spreading resistance in multilayer contacts. The solution is based on the model for the thermal contact resistance between two conforming rough surfaces in a vacuum where an array of circular contact spots is used. The assumption for total thermal resistance of the system consists of two components which are for uniform one-dimensional flow portion (bulk resistance of each layer) and for two-dimensional flow portion which is thermal spreading resistance.

The thermal spreading resistance occurred at the semiconductor junction or coated layer of any surfaces in contact. This is supported by Wing Aung (1991) who explained about the spreading resistance at semiconductor junction. Regarding to the heat flow pattern from the junction through the chip, the heat generated by the silicon chip will spread in three-dimensional manner. Thus, the spreading or constriction resistance is defined as the temperature difference between the average junction temperature and some other reference temperature divided by the total heat flow rate from the junction. The effect of coating technique for circular contact areas to the spreading and constriction resistance has also being considered depend whether on the steady-state or transient condition with uniform heat flux and different boundary condition.

2.2.3 The Finite Element Method in Thermal Contact Resistance.

Trujillo and Pappoff (2002), proposed on the three dimensional finite element methods (FEM) that can be used in thermal contact resistance problem. They provide the solution for the connection of two dissimilar meshes with contact resistance which means that the surface in contact in x-y planes may have their own pattern of nodes and element. The surfaces are assumed to be the contact surfaces between two disconnected three dimensional models and the thermal conductivity assumed to be occurred only in the z direction. Another assumption is that the surface in contact must be labeled with surface A and surface B where surface A must be smaller than surface B. By doing this, the surface A can be projected directly onto surface B. Two dimensional temperature distribution is obtained T(x,y) where z-axis referred to the depth of the element. In overall, this method is used to get the conductance matrix K to represent the heat transfer in z direction. However, the value of thermal contact resistance coefficient has to be determined first and must be included in the formulation. This method can be combined with any suitable thermal contact resistances theory to predict and simulate the thermal resistance at the interfaces.

Grujicic et al.(2004) used the finite element analysis method for a simple model of central processing unit, (CPU) attached to a heat sink to find the contact resistance for the assembly. The CPU used is in cylinder-shape semiconductor surrounded by aluminum heat sink with cooling fins. The thermal model became two dimensional as the heat transfer in parallel direction with the heat sink is neglected. The governing differential equation is used to get the temperature distribution within the CPU/heat sink assembly.

Boundary element method (BEM) is used by Kikuo Kishimoto et al. (1995) in order to analyze the thermoelastic contact problems. This numerical analysis can be divided into two methods. The first method introduced the objective function that can be defined by using residual vectors of discretized boundary integral equations. The solution is found by minimizing the objective function. This method can solved the governing equation of temperature and elastic fields simultaneously. The second method solved the discretized equations of the temperature and stress fields of each body in contact alternately until the satisfied solution for all prescribed boundary condition is found. In overall, BEM method is suitable for contact problem as it considered on the surface roughness. Between the first and second method, the second method used less time for numerical calculation even though the first method that used the objective function treated the couple fields which is temperature and elastic fields simultaneously. For this BEM method, the vector function and its parameters have to be properly considered for different size and material in contact.

2.3 Previous experimental works and the method of applying contact pressure.

Almost all experimental work that has been done to find the thermal contact resistance value considered on the significant factor which always affecting the result that is the contact pressure. Various load used to get the resistance or conductance value at certain pressure. The pressure can be determined first whether in low or high contact pressure range. Li at el. (2000) have studied the effect of loading history from their experimental investigation in vacuum environment. Hysteresis effect has been found where the value of thermal contact resistance when load are increased in ascending manner showed some different when compared with the value of thermal contact resistance when load reduced in descending manner. Besides, the experimental investigation also proved that the number of load cycles and the overloading pressure also improved the thermal contact conductance. All these result can be supported by the mechanical property of the material used based on the theory of elasticity of the asperities. It is found that the thermal contact conductance increased by repeating the loading and unloading method and remained the same at 30 cycles. To get more improved in contact conductance, the overload pressure must be applied and the loading and unloading method can be continued for certain number of cycle until there is no significant effect. Thus, the theory of elasticity is verified.

Milanez et al. (2004) used low contact pressure in their experimental test to compare the result obtained with Truncation Gaussian (TG) method on predicting the hysterisis effect. The hysterisis effect is said to be occured only when high contact pressure is applied where the fully Gaussian method is used to predict the situation. The comparison between TG model and fully Gaussian model with experimental result showed that TG model proposed by Milanez was suitable for low contact pressure, <300kPa. When the contact pressures exceed this value, both TG and fully Gaussian model predicted the experimental data fairly. The TG model referred to the value of z truncated which described the asperity height. The z truncated value must be correlated first by fitting the correlation of the TG thermal contact conductance model for plastic deformation during the first loading.

Wahid and Madhusudana (2000) realized that at low contact pressures, conduction across the gap give a significant effect. Experimental investigation has been carried out where the effect of single and mixtures of gases has been induced to fill the interfacial gas. The gas or interstitial fluids that have been used were helium, argon, carbon dioxide, nitrogen and mixtures of argon and helium. The result obtained has been used to estimate the gap conductance through correlation with three different surfaces roughness.

The effect of overloading and load cycling has been discussed again by Wahid and Madhusudana (2003). The effects supported by experimental test on stainless steel. The experimental method and orientation is almost similar with other previous works. The uncertainty of the test result also has been taken into account. As expected, the hysterisis effect took place for loading and unloading cycles. The overloaded pressure enhanced the contact conductance. For different materials and surface roughness, the number of loading and unloading cycles before overloaded pressure must be applied to get better thermal contact conductance will be varied. Future works for producing reliable theory on loading and unloading effects is recommended.

2.3.1 Observation on the mechanical and surrounding factors in experimental method.

Another important consideration must be made on the test environment. Some of the experimental method provided vacuum surrounding while other testing made under atmospheric pressure. Convection heat transfer will take place around the surfaces in contact. Thus, the heat loss by convection gave significant effect during experiment. Insulator is made by various type of heat resistance material such as calcium silicate and is used to overcome the problem of heat loss made by convection. However, the convection is said to be greater than the convection occurred in vacuum surrounding which can be neglected. Some other assumptions have been made by Wing Aung (1991) in order to develop simple models that can be used to analyze and experimentally verifying the value of contact resistance. Among the important assumptions are the two substrates in contact must be isotropic, radiation is very small and can be neglected and the test surrounding preferably to be vacuum or with continuum interstitial fluid.

Furthermore, the low thermal conductivity of natural gas around and in the interstitial gap also influenced the experimental result. Koichi Nishino et al. (1995) have investigated the value of thermal contact conductance through experiment. As the specimen used is the real material used for space craft component, the accuracy of thermal contact conductance value is needed. They provided vacuum test section where the surrounding pressure is lower than 13.3 Pa which can be said as high vacuum condition as in the outer space. Although the experimental data has been obtained, comparison cannot be done because appropriate theoretical prediction is unused.

Madhusudana (2000) analyzed on the heat transfer uncertainty between contact surfaces during experiment caused by convection, conduction and radiation. The heat dissipation to the surrounding referred to the convection and conduction in the gas surrounding the test column. Radiation factor also must be considered during high temperature where shielding method is the solution. The ratio of surrounding heat transfer to axial heat transfer must be insignificant to ensure that the heat will flow just in one-dimensional which are totally between two contact surfaces. Despite of following the standard method which is ASTM D-5470, consideration must being made on the surrounding of the test section. Thus, vacuum condition provides a good solution for the test section as heat transfer is assumed only by conduction when the ambient pressure below 1 millibar. Furthermore, the flatness deviation which is macroscopic constriction of the contact surfaces also increases the contact resistance. Prediction on those factors affecting the experimental value has been made and compared with the experimental result.

The standard experimental test to measure thermal contact resistance can be obtained from ASTM D5470. Gerald, (2004) described that the standard experimental rigs consist of heater, calorimeter bar, specimen test section, reference calorimeter bar and cooler. Force can be exerted to provide contact pressure to the specimen. There are many ways of applying force to the contact surfaces. Some of them used a bolted nut so that the pressure can be measured by using torque wrench. Load shaft can be mounted on the specimen in axial direction. The load can be applied manually by a load bar or by pneumatic or hydraulic system. The temperature distribution measurement must be made in axial direction in constant distance. At least six calibrated thermocouples must be fixed at the test section. Again, the standard calculation to obtain the temperature at the interfaces is used where these values are extrapolated from the temperature gradient. Heat transfer rate is determined from the energy balances on the heater and cooler. Effective radius of the heater has been discussed by Kutasov and Kagan (2003). They considered on a long cylindrical electrical heater (with a large length/diameter ratio). Assumption in practical case is used where any cylinder whose length is 5 times or higher, then its diameter could be treated as an infinite cylinder. Thus, they considered their heater as an infinite cylindrical source of heat. This study ended with the introduced of an effective radius concept to evaluate the effect of the contact thermal resistance on the heat flow rate into formation. All the experimental data that provide the actual thermal contact resistance value should provide or relate the value of the interface surface roughness. The surface roughness can be mentioned in certain range or in detail. This is the major factor to be used in estimating the high or low thermal contact resistance value. The surface finishing of the interface also can describe the value of thermal contact resistance. Wahid et al. (2003), carried out an investigation to study the effect of surface topography and mean interfacial temperature on thermal contact conductance at a low contact pressure of 0.43 MPa for stainless steel specimen. The experiments have been done in vacuum condition and the interface temperature maintained low. One of the reasons is to ensure that the heat transfer due to radiation across the interface is neglected. Their results showed that the contact conductance improves as the surface roughness value decreases

2.3.2 Steady state condition in thermal contact resistance.

Thermal conduction can be occurred in steady state or transient condition. Rohsenow et al. (1998) in his literature studies has found that the conduction shape factors and thermal contact resistance can be measured in steady state condition. Nazri and Abdullah (2001) have investigated on the effect of contact pressure on thermal contact resistance through experiment. During the experiment, they found that the temperature distribution achieved steady state faster when higher pressure is applied with low heat supply and smooth surfaces specimen involved in the test. For the range of 1.5W to 6.0W with the load range of 0 kg to 6 kg and the surface roughness between 0.9μm to 3.5μm, the time taken to achieve steady state condition is about six to eight hours. This is supported by experimental investigation done by Milanez (2003). For the lowest load, the test achieved steady state after twelve hours while for maximum applied pressure around 3MPa, the time taken to achieve steady state condition is two hours.

2.3.3 Coated layer, Thermal interface materials (TIM) and Phase change materials

Gwinn and Webb (2003) have made an explanation and testing on the TIM characteristic and behavior. TIM can be classified into high and low performance category. Grease and phase change materials are the example of TIM. The ideal TIM must be based on the criteria such as high thermal conductivity, rapid deformation by small contact pressure, thin applied layer, non-toxic, easy to use and constant performance. However, the TIM that suits all these criteria do not exist so far. TIM is most suitable for electronic component for example to improve contact between central processing unit (CPU) with the heat sink. Many disadvantages produced by each type of TIM rather that its benefits. This limits the TIM utilization as mentioned in chapter 1. Test has been done according to the ASTM D-5470 to get the interface resistance of TIM. Steady state condition has been achieved which is suitable for the testing of materials with temperature-sensitive thermal and mechanical properties like TIM. The test section has been insulated. The test produced unreliable result to be compared with actual application in electronic component due to TIM high sensitivity.

Coated layer

Another method to increase the thermal contact conductance or resistance is by using the coating method. The thermal conductivity value of the coating layer must be greater then the value of the substrate in order to improve the thermal conductance or in different way, the value must be lower to increase the thermal resistance. Marotta et al. (1999) examined the appropriate of using the already developed theoretical model to predict the thermal contact conductance of sintered copper coatings on ferro-alloy. The prediction is made to compare with his experimental works on this coated alloy. The experimental investigation has been made at the pressures of 2.5 to 25 MPa with different sinter copper coating thickness. The tests were made at mean interface temperature for appropriate comparison. The results obtained for some copper coating thickness and base materials that have been test to suits some of the condition for example the interface pressure that exist at a valve seat/engine block interface of internal combustion engine. For plastic deformation model of the coated layer, the theory of Antonetti and Yovanovich has been used to compare with the test result while for uncoated surfaces; prediction has been made by the correlation from Cooper, Mikic and Yovanovich, (CMY). The CMY correlation prediction showed less scatter compared with Antonetti and Yovanovich. In overall, both theories unable to predict the coated and uncoated layer of sintered copper coatings on ferro-alloy due to some factors such as material composition, interface porosity, and anisotropic surface roughness.

2.3.4 Thermal contact resistance test on different materials and purposes

Ponnappan and Ravigururajan (2004) have carried the experimental investigation on Li-ion batteries. It is showed that the resistance increases with decreasing pressure and the effect is significant when the pressure is reduced below 689.5 kPa. They also found that hot spot occurred on the layer of separator when the temperature increased beyond 80°C. The hot spot caused contact between anode and cathode and thus deteriorate the battery. Their tests where conducted in both wet and dry condition (with and without immersed in the electrolyte). However, one major assumption in all experimental method is that the transport properties are independent of temperature and pressure.

Ismail et al. (2004) have repeated the experimental investigation on Li-ion cell battery where experimental study used to determine the thermal contact resistance at the contact pressure of (30-130kPa) in dry condition. The contact pressure used to see the decreased in thermal contact resistance. The surface roughness of the materials also have been measured and used to obtain the thermal contact resistance by theoretical calculation. The theoretical prediction showed very much different value of thermal contact resistance compared to the experimental result. The rough surfaces of anode and cathode produced high thermal contact resistance value while the low thermal conductivity of polyethylene/polypropylene (PEPP) was probably the reason for high thermal contact resistance value for separator. In conclusion, the same trend of the previous result on Li-ion battery has been obtained.

Parihar and Wright (1997) examined the thermal contact resistance and total resistance at elastomer to metal interfaces. They found that for common thickness silicone elastomer (4.76mm), the interface resistance between metal-elastomer-metal contacts is about 25% of total resistance. The percentage of interface resistance caused by elastomer will be increased and become dominant when the thickness reduced < 2mm. At the upper interface, the heat flow lines in the metal asperities are constricted due to the low value of elastomer thermal conductivity while at the lower interface, the heat flow lines constriction reduced as lower the metal specimen act as a cooler or heat sink. They concluded that the intensity of the constriction or spreading of the heat flux lines between the interfaces depends on the intensity of the surface irregulaties, deformation of the softer material, the ratio of thermal conductivities of the materials in contact and the direction of heat flux. The importance of this study based on the used of elastomer such as gaskets and seals for mechanical joint.

Yeh and Lin (2003) have studied on the thermal contact resistance correlation for metals across bolted joints through experimental test. Three types of specimens were used, including aluminum, copper and stainless steel. The result showed that the contact pressure increased when the number of bolt applied to joint the specimen increased. Furthermore, the torque applied to the bolt also increased the contact pressure. The contact pressure is measured by pressure-measuring film where the color concentration on the film can described the torque applied. The surface roughness of the square plates and their different thermal conductivities value also gave significant effects on experimental results. Two dimensionless numbers have been produced based on interfacial contact pressure. Dimensionless pressure P^* include the function of the modulus of elasticity and Poisson's ratio for two contacting surface while dimensionless torque, τ^* contained the yield strength of the bolts and the combines rms surface roughness of two contacting surfaces. The experimental observation produced two dimensionless group which are dimensionless resistance R^* and P^*. Finally the resulting correlation between these two dimensionless groups is presented. The uncertainty analysis also has been done.

Chung et al. (1995) studied on the ceramic substrate that often used in microelectronic packaging since the first integrated circuit, IC was introduced. The study is made through experiment to obtain thermal contact conductance at ceramic junction. The test involved alumina substrates in contact with aluminum which often used as a heat spreader for IC. The ceramic substrate then has been coated to improve the contact conductance and test in their experiment. Copper, aluminum, iron carbide, and copper plus aluminum coatings have been applied to the ceramic surfaces. The effect of surface roughness also has been monitored. Significant improvement in the thermal contact conductance was observed for the copper plus aluminum coated ceramic substrates. The uncertainty during experiment has been recognized from the temperature drop caused by temperature readings and the extrapolated temperature.

Yeh et al. (2002) investigated the thermal contact resistance of aluminum honeycomb. The honeycomb is always used as a lightweight structure, such as for space craft, aircraft, satellite, and high-speed trains. There are many advantages of using this honeycomb due to their mechanical and thermal characteristics. Compact heat exchangers, solar collectors, thermal insulators and catalytic burners are the examples which used the honeycomb as part of its components. Their studies concentrated on the hexagonal shape of honeycomb with different size and high. The anisotropic nature of honeycomb structures caused the difficulties to predict the heat conduction mechanism across the honeycomb. The experiment has been done in atmosphere to get the thermal contact resistance of honeycombs sandwiched by two aluminum blocks. Their objectives of study are to observe the effect of honeycombs specimen specification and joint condition on the heat conduction properties. The parameters included the cell size, height and material type. The influence of interfacial contact have been found by manipulating the experiment procedure such as the orientation of the honeycombs in axial and lateral position, variation number of bolts used, bolts sizes and torque applied with different joint pattern. The result showed that the thermal contact resistance between solid aluminum surface and a lateral honeycomb is larger than the honeycombs in axial orientation. The number of bolt and the higher torque increased the thermal contact conductance respectively.

Very low thermal contact resistance is needed for the experiments at ultra low temperatures below 1 mK. The test suits the quest for the anticipated of lithium metal superconductivity at milikelvin regime. A brief report has been made by Juha Tuoriniemi et al. (2003) which stated that another objective of studying the thermal behavior of Lithium metal is about its nuclear magnetism. Their complex test has been done to find the best material that can be used to capsulate the lithium for their next investigation. They found that silver and gold were not suitable to capsulate the lithium in their low temperature experiments according to early mixing with the metals at room temperature. Copper is the best material to capsulate the lithium if used with good diffusion welding.

Copper based Metal Matrix Composites (MMCs) reinforced by carbon fibers can be described as the combination between high thermal conductivity material with a low coefficient of thermal expansion (CTE). The used of this composite is limited because of the weak mechanical bonding between the carbon fibers and copper. Neubauer et al. (2003) focused on the investigation of mechanical and thermal interfacial properties of this composite material. A glassy carbon with very smooth surface has isotropic properties. Thus the macroscopic surface roughness parameter is neglected. As the adhesion between copper and carbon became the problem for this composite, the mechanical adhesion have been prepared with different methods and tested by pull-off method. Each of the adhesion strength has been recorded where copper coating with Ti layer on cleaned substrate has the strongest bond between layers. The measurement of the thermal transport properties and the determination of the thermal contact resistance are done by using a photothermal system instead of thermocouples. This is s special method to measure the temperature distribution between the layer interfaces. It is made by enabling excitation and detection of the thermal waves in the heating modulation frequency range of 0.01 Hz<f<100 kHz. The thermal wave amplitude versus function of frequency measured at an average sample temperature of approximately 25°C has been recorded together with the value obtain by the composites. The measurement of the thermal waves produced thermal transport properties between copper coatings and carbon substrates. Thus, correlation between the thermal contact resistance and the mechanical adhesion strength also derived. It is found that the better the mechanical adhesion between these composite layers or the stronger the bonding, the lower the thermal contact resistance between the composite layers interfaces.

ElSherbini et al. (2003) investigated on the thermal contact resistance in plain-fin-and tube evaporators with collarless fins. This tube is widely used as heat exchanger in refrigeration systems. The overall thermal resistance of this tube also can be affected by the thermal contact resistance at the interface between fins and tubes. Fins and tubes contact mostly attached by inserting the tubes into the fin stack and expanding them by mechanical method or by hydraulic or pneumatic pressure. This method caused the elastic or plastic deformation of the tubes and fins and allowed the elastic relaxation. Some other method used to attach the fins and tubes by pressing or brazing the joint.

ElSherbini and co-workers did the experiment in a closed-circuit wind tunnel and tested two geometrically identical heat exchangers with 8 rows and 2 columns of tubes. Inlet and outlet air temperature have been measured. Two conditions have been considered which were in dry and frost condition. An energy balance between the air and coolant streams was used for reference. The heat exchanger performance has been analyzed considering the uniform convection heat transfer coefficient throughout the heat exchangers. Some equation has been derived from thermal resistance network of the heat exchangers which finally produced the overall thermal conductance of the heat exchangers. After considering the experiment uncertainty, the results showed that the thermal contact resistance effect can only be found in dry condition. The unbrazed fins and tubes gave high thermal contact resistance value rather than brazed fins and tubes as expected. The aluminum brazing method improved the contact between the fins and tubes but the cost constraint due to the number of fins must be considered. However, under frost condition, unexpected result has been occurred where the brazing method is not necessary. The value of thermal contact resistance for both brazed and unbrazed joint were almost same as the frost maybe improved the thermal contact for the unbrazed tubes and fins.

Nakayama and Bergles (2003) reviewed on the application of thermal interfacing techniques for electronic equipments. The trend of thermal contact resistance problems and the solution has been discussed with concentrated on the electronic fields. As the reduced in sizes and spaces of electronic equipments, the heat transfer finally must be modeled to the traditional ways such as natural convection and radiation. The contact pressure constraint of electronic components leads to the used of many thermal interface materials such as heat spreader, thermal grease and so on. They have concluded some issues related to the thermal interface management for electronic equipment.

The major factor for the effectiveness of interface management based on the range of allowable contact pressure on the electronic device and other thermal resistance components in the heat transfer route.The heat transfer of thermal contact conductance investigated from experiment always considered on high contact pressure ranges-higher than 0.5 MPa. More experiments have to be conducted with low contact pressure (0.1-0.5 MPa) to suits the actual environment in electronic devices. Macroscopic surface characteristic occurred in the thermal interface technique such as warping and corrugation have to be considered together with microscopic parameters that is the surface roughness. Many compact and portable electronic devices thermal management focused on the efficient heat spreading in narrow spaces. This showed that in compact equipment the thermal interface management has to be an integral part of the overall design of heat transfer paths from the heat source to ultimate heat sink.

CHAPTER THREE

THEORETICAL PREDICTION FOR THERMAL CONTACT RESISTANCE

3.0 Introduction

Theoretical prediction has been made to predict the thermal contact resistance between surfaces in contact. The prediction is based on the actual specimen used in the experiment. The plastic contact resistance model of Cooper, Mikic and Yovanovich is used. The theory for elastic deformation from elastic contact conductance models of Mikic and Greenwood and Williamson also has been revised. However, the elastic theory is not valid for low contact pressure. The value of contact heat transfer coefficient can be predicted by these models. The estimation of actual contact area also provided from the model. Since only low contact pressure applied in the experimental test, the model seems suitable for aluminum which may experience plastic deformation under low contact pressure. This can be approved by the prediction values discussed in chapter five.

3.1 Gaussian distribution of the asperity height and slopes.

For any surface undergo grind or grit-blasted process, the distribution of asperity heights is rather close to Gaussian although the height of the asperity is random (Greenwood and Tripp, 1970). Such as in this experimental research, the specimen surfaces have been ground and polished. The advantage of this method is when the Gaussian height distribution is considered, the mode of deformation, asperity shape and whether the asperities are on one or both surfaces are not important. $P(Z/\sigma)$ are the surface asperity probability distribution while Z is the asperity height. Figures 3.1 and 3.2 described the surface asperity height and the geometric parameters.

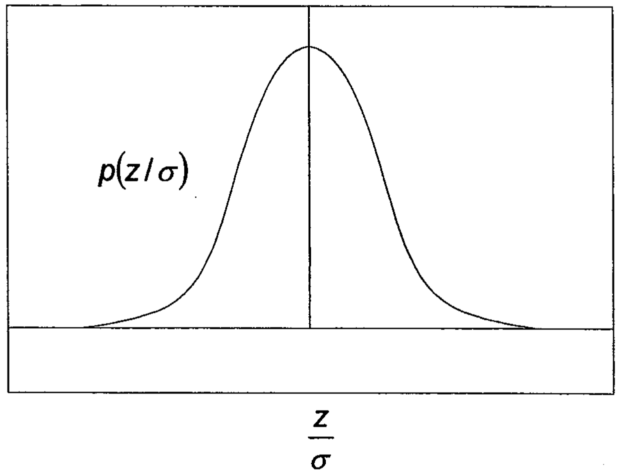

Figure 3.1 Asperity height distributions by Gaussian Model

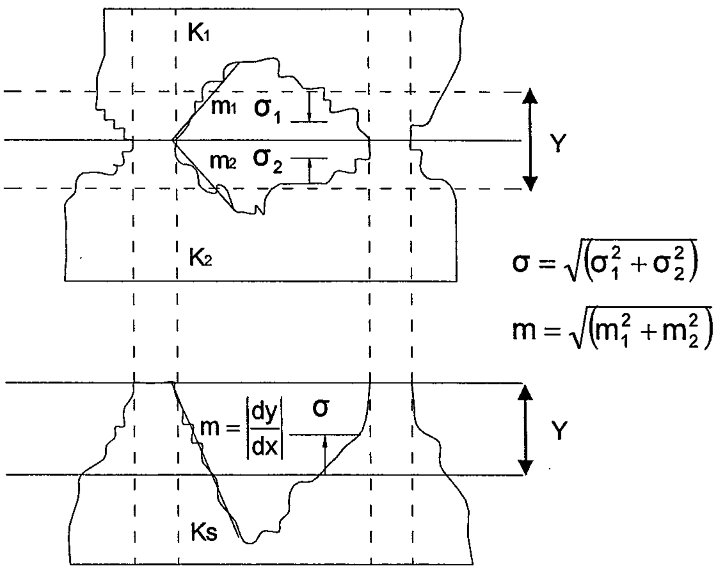

Figure 3.2 Conforming rough surface geometric parameters

3.2 Plastic Contact Resistance Model of Cooper, Mikic and Yovanovich.

The plastic model of Cooper, Mikic and Yovanovich (CMY) has been used to predict the thermal contact resistance and compared with the experimental result. Aluminum has been predicted by this theory according to the plastic deformation under low contact pressure. The CMY model is based on Gaussian distribution of the asperity height and slopes, the plastic deformation of the contacting asperities, and the constriction resistance that based on the isothermal circular contact area on a circular flux tube result. The simplified equations that have been derived for conforming rough surfaces were given below;

Conductance dimensionless coefficient

$$Cc = \frac{\sigma}{m} \cdot \frac{h_c}{K_s} = \frac{1}{2 \cdot \sqrt{2\pi}} \cdot \frac{\exp\left(-x^2\right)}{\left(1-\varepsilon\right)^{1.5}} \tag{3.1.1}$$

With x and ϵ is given by,

$$x = erfc^{-1}\left(\frac{2P}{H_c}\right) \tag{3.1.2}$$

and

$$\varepsilon = \sqrt{\left(\frac{P}{H_c}\right)} \tag{3.1.3}$$

The $erfc^{-1}$ value must be selected from the error function table. This value also can be estimated by using the equation below as mentioned by Song and Yovanovich (1998).

$$erfc^{-1}\left(\frac{2P}{H_c}\right) \cong 0.9638\left[-\ln\left(5.589\frac{P}{H_c}\right)\right]^{\frac{1}{2}} \tag{3.1.4}$$

This equation is valid for the range given below;

$$10^{-6} \le \frac{P}{H_c} \le 2\times10^{-2} \tag{3.1.5}$$

It is found that for aluminum under contact pressure between 34kPa-132KPa and with Vickers microhardness (HV) 470.4 MPa, the range is satisfied. The contact microhardness is complex. The value of contact microhardness depends on geometric and physical parameters, such as the Vickers microhardness correlation coefficients, c_1 and c_2. The contact microhardness equation is as given below as given by Rohsenow et al (1998);

$$\frac{P}{H_c} = \left[\frac{P}{c_1(1.62\sigma / m)^{c2}}\right]^{\frac{1}{1+0.071c_2}} \tag{3.1.6}$$

And c_1 and c_2 are as follows;

$$\frac{c_1}{3178} = \left[4.0 - 5.77H_B^* + 4.0(H_B^*)^2 + 0.61(H_B^*)^3\right] \tag{3.1.7}$$

$$c_2 = \left[-0.370 + 0.442\left(\frac{H_B}{c_1}\right)\right] \tag{3.1.8}$$

The Vickers microhardness value also given as follows;

$$H_v = c_1 d_v^{c_2} \tag{3.1.9}$$

Where d_v is the mean indentation diagonal in μm, c_1 and c_2 are the correlation coefficients. In the calculation of contact microhardness, assumption that has been made is the contact microhardness of the surface being penetrated by the asperities of the harder surface is the same as the the vickers microhardness corresponding to the equivalent Vickers indentation diagonal;

$$H_c = c_1 d_v^{c_2} \tag{3.1.10}$$

For the surface parameters such as surface roughness, σ_1 and σ_2 with RMS values and absolute mean slopes of the surface asperities of the contacting surfaces, m_1 and m_2 were given below;

$$\sigma = \sqrt{\left(\sigma_1^2 + \sigma_2^2\right)} \tag{3.1.11}$$

$$m = \sqrt{\left(m_1^2 + m_2^2\right)} \tag{3.1.12}$$

The mean absolute asperity slope can be approximated by the correlation equation proposed by Antonetti as revised by Yovanovich et al (1997) which was valid for the surface roughness range of 0.216 $\mu m \leq \sigma < 9.6\ \mu m$.

$$m = 0.125\ (\sigma \times 10^6)^{0.402} \tag{3.1.13}$$

The interface effective thermal conductivity is defined as;

$$k_s = \left(\frac{2k_1 \cdot k_2}{\left(k_1 + k_2\right)}\right) \tag{3.1.14}$$

The contact conductance equation has been modified to obtain the heat transfer contact coefficient as mentioned below from the original CMY model. By substituting all the values into this equation, the heat transfer contact coefficient can be calculated by using;

$$hc = \frac{m \cdot k_s}{\sigma} \cdot \frac{1}{2\sqrt{2\pi}} \cdot \frac{\exp\left(-x^2\right)}{\left(1-\varepsilon\right)^{1.5}} \tag{3.1.15}$$

Then, the values were substituted into the equation below to obtain the TCR value;

$$h_c = \frac{(Q/A)}{\Delta T_c} \tag{3.1.16}$$

The thermal contact resistance (TCR) prediction equation;

$$R = \frac{1}{h_c \cdot A} \tag{3.1.17}$$

3.2.1 The estimated real contact area from CMY model

The estimated real contact area is based on the CMY model. The metrology model gives the geometric relationship as follows;

Relative real contact area.

$$\varepsilon^2 \equiv \frac{A_r}{A_a} = \frac{1}{2} \cdot erfc(x) \tag{3.2.1}$$

As the specimens used based on the isothermal circular contact area on a circular flux tube result, the nominal contact area is given as below.

$$A_a = \pi r^2 \tag{3.2.2}$$

3.3 Elastic Contact Resistance Model of Mikic and Greenwood and Williamson.

The dimensionless contact conductance equation obtained from Elastic Contact Resistance Model of Mikic and Greenwood and Williamson can be used to get the thermal conductance as described below where parameters such as surface roughness, σ and absolute mean slopes of the surface asperities of the contacting surfaces, m must be used.

$$hc = \frac{m \cdot k_s}{\sigma} \cdot 1.54 \left(\frac{\sqrt{2}P}{mE'} \right)^{0.94} \tag{3.3.1}$$

However, under low contact pressure, this equation is not suitable. This equation has been developed for the ranges of $10^{-5} \leq \dfrac{\sqrt{2}P}{mE'} \leq 10^{-2}$. Thus, this theory is not used to calculate the elastic factor as the study concentrated on low contact pressure which was below 132kPa. The suitable contact pressure for this elastic model prediction to be used for hard materials such as stainless steel is above 311kPa which is three times higher that has been used in this study. Aluminum mostly experienced surface asperity plastic deformation while brass, mild steel and stainless steel surface asperity are more related to the elastic or elastoplastic deformation.

CHAPTER FOUR

EXPERIMENTAL LAYOUT

4.0 Introduction

The present research works are concentrated on the experimental test to obtain the thermal contact resistance. The experimental rig has been developed in order to provide suitable condition for the experimental test. The rig is made according to the standard model, ASTM D-5470, which is used to determine thermal contact resistance. The salient parts of the rig are mentioned below. For thermal conduction test, the energy balanced became important to provide the steady state condition. The thermal and cooling system must be developed for proper heat flow through the test specimen. The specimens used are also discussed. In the end of this chapter, the data and error measurement has been estimated to obtain the uncertainty of the experimental results. The experimental rig is shown in Figure 4.1.

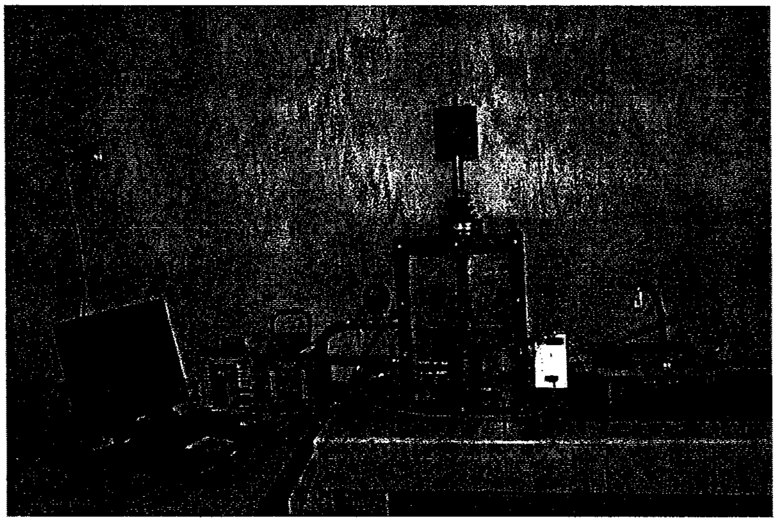

Figure 4.1 The experimental rig

4.1 Development of test rig apparatus

The experimental rig is made for both ambient and vacuum environment. The test rig can be described as a rectangular box made by transparent perspex material. This transparent material allowed the monitoring of the specimen and thermocouples position that must be fixed during experiment. The detail of experimental rig system used in ambient surrounding is shown in Figure 4.2. The rig experimental diagram has been labeled from 1-12.

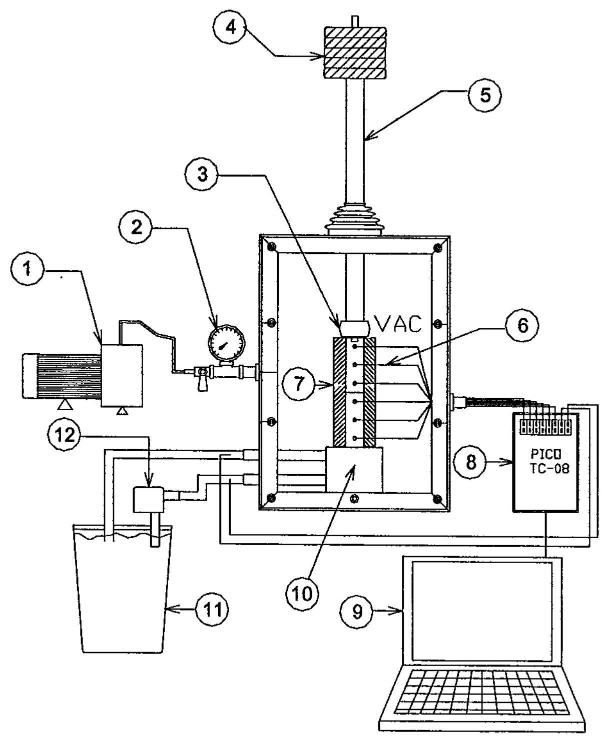

Figure4.2 Experimental rig diagram

The diaphragm vacuum pump (1) has the ultimate vacuum pressure of -75kPa. The vacuum gauge (2) mounted at the right side of the rig is used to monitor the vacuum pressure. The heater (3) is a ring type with a suitable diameter to be clamped at the brass shaft. The box is equipped with weight block (4) and load supporter brass shaft (5). A set of type K thermocouples (6) is mounted at the box together with the control of data acquisition. To avoid from heat losses caused by convection, a baked ring made by calcium silicate (7) is used to ensure that the specimen will be fully insulated. The PICO TC-08 data acquisition (8) is used and connected to a computer. A VAC power supply used to control the heater. The data acquisition connected via computer (9) to monitor the temperature distribution. Heat sink compound was applied to reduce the contact resistance between heater and chiller. Hollow cylindrical brass block acted as a chiller (10). The cooling water tank (11) and water circulation pump (12) has been used to obtain steady state condition during experimental test.

4.1.1 The important parts of the experimental rig.

A few important parts have to be considered in the development of the experimental rig especially for the vacuum test. The structure, thermal and cooling system, data acquisition and vacuum pump are among the salient parts. The rig structure of the vacuum chamber is shown in Figure 4.3. It is made by mild steel angle bar and properly welded into the rectangular box shape. This rig structure is made to support the outside rig wall from atmospheric pressure when the internal pressure is reduced. It is made by stainless steel plate with 1.5 mm thickness and welded to the rig structure.

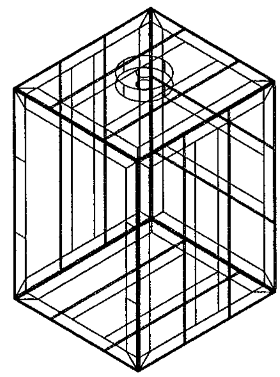

Figure 4.3 The rig structure

The side wall experienced compression and decompression when repeating the experimental test. Thus, the rig is designed with two supported angle bar at each side of the rig structure and the stainless steel side wall are welded to the angle bar in order to reduce the compression and decompression phenomena. A manual load used to increase the contact pressure on the contact surfaces. The load used is 1kg cylinder block. Five pieces of block are used and provided total pressure of 132kPa approximately. For temperature measurement, eight pieces of type K thermocouples are used and plugged to the PICO TC-08 data logger. This temperature data acquisition provides eight channel readers. Six thermocouples used to measure the temperature distribution at the specimen while another two thermocouples used to monitor the inlet and outlet water temperature.

4.1.2 Thermal and cooling system.

A simple thermal and cooling system is built. The most difficult was to obtain the steady state condition. Heater provides heat to the specimen and the heat flow between the surfaces in contact while brass hollow block acted as a chiller. The water was used to flow inside the block as a cooling medium. The heater power is supplied by AC voltage regulator where the voltage is set at 50 V for the entire experimental test. As the specific heat of water, Cp was very high (4200 J/kg K), the different between outlet and inlet water temperature was very small. An energy balance can be made when the experimental test achieve steady state. As the time taken to achieve steady state condition depend on many factors such as the contact pressure and the heat supply, the estimated time has been used for every experimental test.

Table 4.1 The Heat value from experiment

Approximate heat, Q from experimental results								
	aluminum		brass		mild steel		stainless steel	
Contact Pressure (kPa)	Q_1	Q_2	Q_1	Q_2	Q_1	Q_2	Q_1	Q_2
34.82	3.077	3.663	4.227	3.556	2.803	1.958	1.090	1.179
54.16	3.069	3.735	4.238	3.564	2.895	1.964	1.069	1.178
73.51	3.122	3.762	4.239	3.312	2.860	1.952	1.068	1.174
92.85	3.180	3.812	4.240	3.222	2.869	1.973	1.077	1.170
112.19	3.181	3.933	4.198	3.273	2.823	1.901	1.091	1.169
131.54	3.250	4.020	4.236	3.224	2.843	1.943	1.105	1.163
Q Mean	3.147	3.821	4.230	3.359	2.849	1.949	1.083	1.172

An energy balance is made by measuring the inlet and outlet cooling water temperature. Table 4.1 showed the heat flux of the specimen's material.

The different between outlet and inlet temperature value is used to get the value of heat absorbed by the chiller. The heat value indicated the constant heat supplied to the specimen by the heater. It is measured by using the equation below. The heat flow rate also can be compared with the calculation of the temperature gradient between the two specimens in contact. The value of heat flow through the test specimen compared with the heat absorbed by the cooling water is shown in the Table 4.2 below. The results obtained from two sample test of aluminum. From the results shown, the heat flow from the specimen to the cooling water can be described in steady state where it is not much differed.

Table 4.2 Heat absorbed by the specimen and cooling water for aluminum

Q1 specimen	4.42W	Q1 water	5.74W
Q2 specimen	4.34W	Q2 water	4.15W
Q specimen (mean)	4.38W	Q water (mean)	4.95W

4.1.3 Specimen preparation

Four different types of specimen are used for major test. The specimens have been machined into solid cylindrical shape with 50 mm long and 25.4 mm in the diameter approximately. Slots are made at upper and lower specimens in order to fix the specimen position as shown in Figure 4.4 and 4.5. The materials used are stainless steel, brass, mild steel and aluminum. They can be classified as hard and smooth material according to their hardness. The materials properties such as surface roughness and surface hardness have been measured while other information referred to the Online Material Properties website (2005) as shown in the Table 4.3.

Table 4.3 Specimen thermal and mechanical properties

Specimens	Thermal Conductivity (W/mK)	Nominal contact Area (m^2)	Vickers microhardness (HV)	Young's Modulus (E) GPa
Aluminum	204	5.07×10-4	48.0	70
Brass	111	5.07×10-4	146.9	115
Mild Steel	48.5	5.07×10-4	157.1	200
Stainless Steel	15.1	5.07×10-4	286.5	200

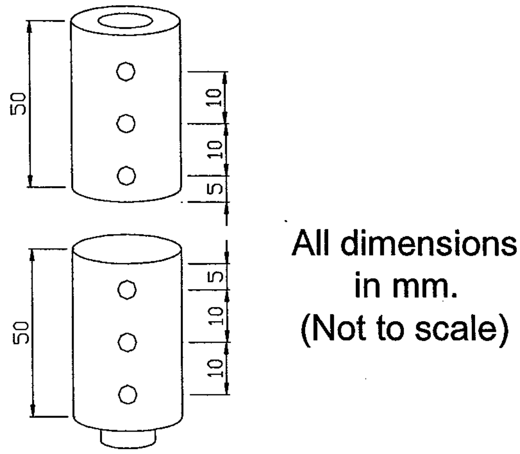

Figure 4.4 Specimen dimension and thermocouples location holes.

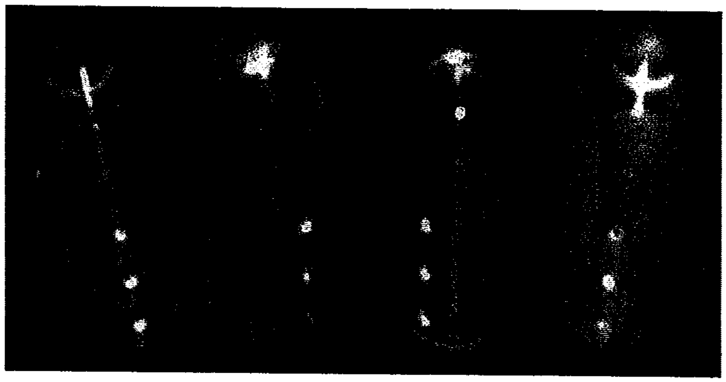

Figure 4.5 The different types of specimen

The specimen surfaces have been ground and polished using grinding machine. The surface rouhgness has been measured using Mitutoyo Surftest SV-210P profilometer as shown in Figure 4.6 while the surface microhardness is measured by Mitutoyo Vickers Microhardness Measurement unit.

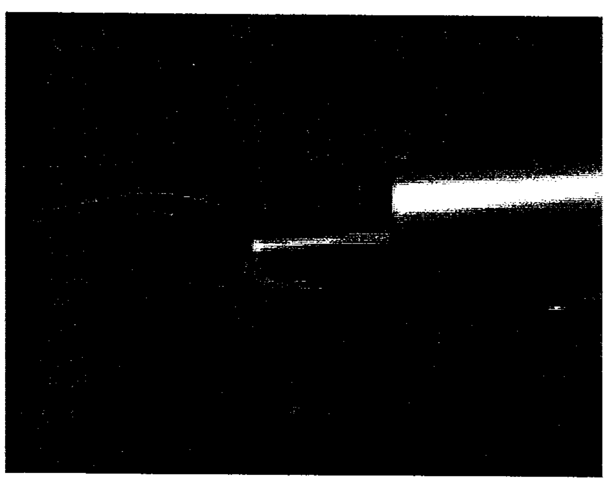

Figure 4.6 Measuring the Surface Roughness

4.2 Experimental set up and testing procedures.

The experiment has been repeated for four different specimens with upper portion-lower portion coordination. The experimental procedures are mentioned below;

- Each of the specimens surfaces has been ground and polished in order to obtain the smooth surface (<1.0μm) and rough surface (>1.0μm).
- The specimen is mounted in axial direction where the upper specimen fixed with the load shaft and the lower specimen fixed on the chiller block. The contact between upper and lower specimen surfaces must be ensured flat to get the real value of nominal contact area. The test assembly as shown in Figure 4.8.
- Six thermocouples are inserted into the holes drilled at the side of upper and lower specimen according to the same distance between each other starting from upper to lower portion with marks T1, T2, T3, T4, T5 and T6.
- For ambient environment test, the specimen has been fully insulated.
- The temperature measurement is taken by data acquisition connected via computer. It is taken after (8 hours or 400 minutes) of experiment when it reached a ***steady state condition.*** (Nazri and Abdullah, M.Z (2001)) and can be referred to Figure 4.8.
- The opening wall of the rig must be tightly closed. This has been made by clamping the Perspex wall with bolts and nuts. The vacuum pump must be run until it achieved the ultimate vacuum pressure. It is followed by turning on the heater power supply and cooling water pump. The 50V voltage power is supplied.

- Water has been pump into the chiller to be the cooling medium during experiment.
- During the experimental test, the thermocouples reading must be monitored from time to time. The data or the thermal system of the experimental rigs can be validated from the temperatures reading.

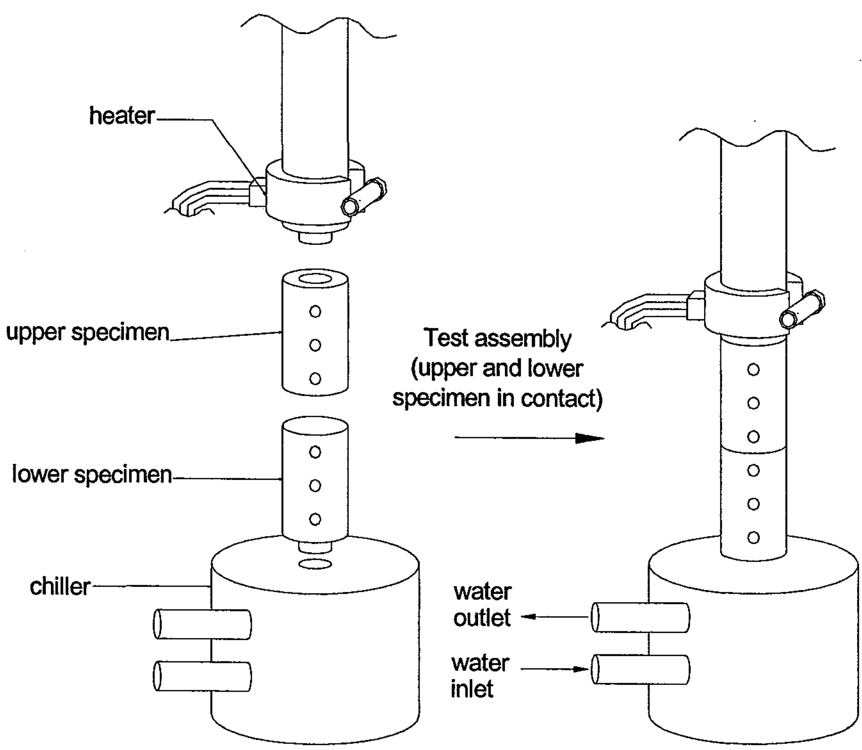

Figure 4.8 The test assembly

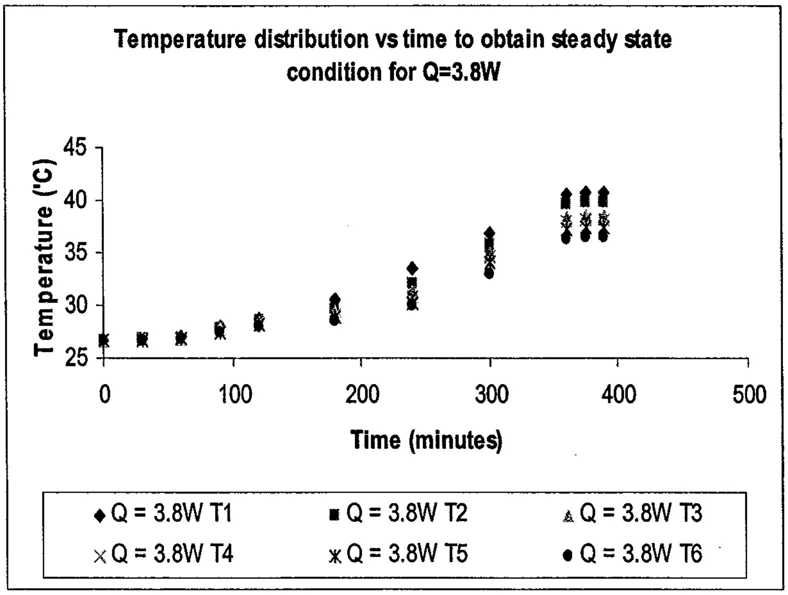

Figure 4.9 The temperature distribution obtained by Nazri and Abdullah, M.Z (2001))

From the graph in Figure 4.9, it is shown that the temperature distribution achieved constant value or steady state after 400 minutes of experiment when the contact pressure between 34.2 kPa to 132 kPa is applied. T1, T2, T3, T4, T5 and T6 are the thermocouples readings used in the experiment.

4.2.1 Test procedure for Li-ion cell battery layers (dry test)

The layers have been cut into cylinder shape with 25.4 mm diameter size. The battery sample and the layer arrangement can be seen in Figure 4.9 below. The experiment repeated for four different arrangement of the specimen as listed below;

1) Plain brass rod: (upper portion-lower portion).
2) Graphite coated copper anode film sandwiched between brass rods: (brass-anode- brass).

3) Lithium cobalt oxide coated aluminum cathode film between brass rods: (brass-cathode-brass).

4) PEPP separator film between brass rods: (brass-separator-brass).

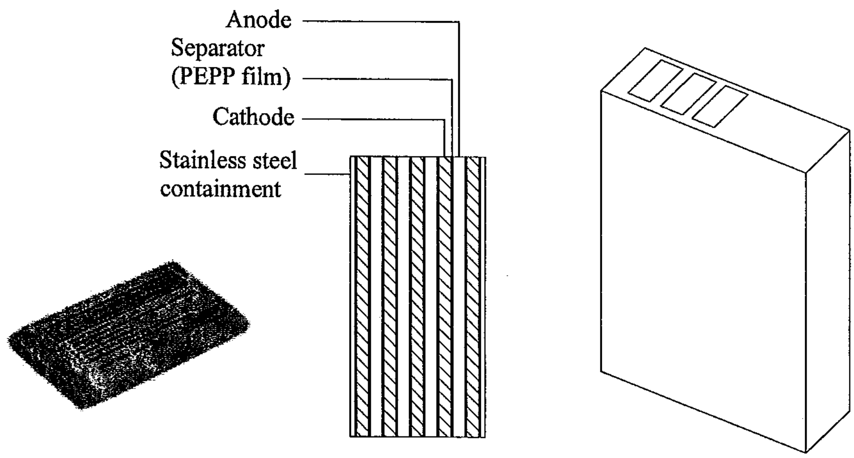

Figure 4.10 The Li-ion battery and cross section of electrode layers.

4.3 Data and uncertainty measurement of the experimental result

Six temperature values at different location on the specimens have been obtained and recorded in the computer. The temperature values were then plotted on the temperature versus distance graph where the extrapolated values at the interfaces can be found using the Fourier's Law. Table 4.4 showed the data samples and data error measurement. The error measurement or uncertainty of the experimental result has been estimated by using aluminum test data. Due to the time and cost constraint, the repeatability has been limited for two to three samples. The method used was based on Section7, Step 4, Calculating the Combined Uncertainty (2005). They mentioned that for the uncertainty components which evaluated experimentally, from dispersion or repeated measurement, the uncertainty value can be directly obtained as standard deviation of the data. The combined uncertainty equation can be mentioned in equation 4.1.1.

$$U_c(TCR) = TCR\sqrt{\left[\left(\frac{u(\Delta T)}{\overline{\Delta T}}\right)^2 + \left(\frac{u(Q_{ave})}{\overline{Q}_{ave}}\right)^2\right]} \tag{4.1.1}$$

Table 4.4 Measurement parameter for aluminum specimen

Sample	Specimen ΔT drop At 112 kPa	$\frac{dT}{dx}top$	$\frac{dT}{dx}bott$	$\frac{dT}{dx}ave$	Water ΔT drop At 112 kPa	Water flowrate m^3/s
1 2 3	1.480 1.166 0.966	 40.67 40.17	 45.08 46.67	 42.88 43.42	 0.07 0.05	2.00×10^{-2} 1.80×10^{-2} 1.90×10^{-2}
Mean	1.16	40.42	45.88	43.15	0.06	1.9×10^{-2}
Standard deviation/ uncertainty	0.26	0.35	1.12	0.38	0.014	1×10^{-3}
Combined uncertainty	$TCR = \frac{\Delta T}{Q_{average}}$ $U_c(TCR) = 0.052 \approx \pm 5\%$					

It is shown that the overall uncertainty estimation of the experiment is $\pm 5\%$. The temperature gradient for upper and lower specimens indicated the heat transfer rate. Value of thermal contact resistance from experiment was obtained by calculation as mentioned in equation 4.1.2 and 4.1.3.

CHAPTER FIVE

RESULT AND DISCUSSION

5.0 Experimental result overview

Generally, all the specimens experienced the thermal contact resistances in the experimental test. It showed that the thermal contact resistance (TCR) reduced by increasing the contact pressure for all specimens. Low contact pressure has been used approximately in the range of 34 kPa to 132 kPa. In this study, the specimen surface roughness, the test environment, the contact pressure and hardness of the materials are among the important parameters that have been discussed. In addition, the comparison between the plastic model of Cooper, Mikic and Yovanovich (CMY) has been used to compare with the experimental results. The thermal contact resistance in Li-ion cell battery also has been made. For Li-ion cell battery, the thermal contact resistance between various layers of the cell stack is the important factor whenever it is extremely used (Rengasamy and Ravigururajan, 2004). This experimental test has been made in dry condition which means that the battery electrode layers are not immersed with electrolyte. The test on the battery electrode layers is to describe the capability of the experimental rigs to investigate the thermal behavior for many cases such as in electronic equipments that experienced the thermal contact resistance problems.

5.1 Effect of surface roughness to the temperature drop between contacting surfaces.

Surface roughness is among the important parameters that affect the thermal contact resistance value. The table below showed the results for aluminum, mild steel, brass and stainless steel based on their surface roughness.

Table 5.1 The different between smooth and rough surface in thermal contact resistance value.

Thermal contact resistance (°C/W)							
aluminum		mild steel		brass		stainless steel	
smooth surface	rough surface	smooth surface	rough surface	smooth surface	rough surface	smooth surface	rough surface
0.127	0.398	0.180	2.844	0.131	0.334	0.366	1.433
0.128	0.386	0.171	2.819	0.131	0.331	0.365	1.416
0.125	0.385	0.173	2.811	0.129	0.332	0.367	1.417
0.123	0.380	0.165	2.795	0.128	0.326	0.358	1.422
0.127	0.376	0.159	2.835	0.126	0.328	0.353	1.396
0.112	0.373	0.151	2.750	0.126	0.329	0.353	1.396

It is significantly showed in Table 5.1 that the surface roughness increased the thermal contact resistance for all specimens. The higher the surface roughness value, the higher the thermal contact resistance between two surfaces in contact. In the sub-chapter of 5.1.1 and 5.1.2, the smooth and rough surfaces have been discussed separately.

5.1.1 Effect of smooth surface to the temperature drop at the interfaces

In this study all the four specimens have been ground and polished to obtained smooth and rough surfaces. In Table 5.2, the surface roughness value of the specimen has been given. The upper and lower specimens have the roughness value below 1 μm. It is assumed that the specimens with surfaces roughness δ_1 and δ_2 approximately below 1.0 μm are considered as smooth surfaces while the values above 1.0 μm assumed to be rough surfaces.

Table 5.2 Specimens surface roughness (smooth).

Spesimen	Specimens surface roughness (μm)					
	R_q (in vacuum)			R_q (in ambient)		
	δ_1	δ_2	δ	δ_1	δ_2	δ
aluminum	0.65	0.46	0.80	0.19	0.19	0.27
brass	0.96	0.69	1.18	0.39	0.34	0.52
mild steel	0.79	0.69	1.52	-	-	-
stainless steel	0.84	0.65	1.98	0.45	0.55	0.71

Figures 5.1, 5.2 and 5.3 described the temperature drop at the interfaces in vacuum condition. Temperature drops at mating surfaces have been measured from the extrapolated value of the temperature gradients. It is measured by subtracting the temperature value at the interfaces.

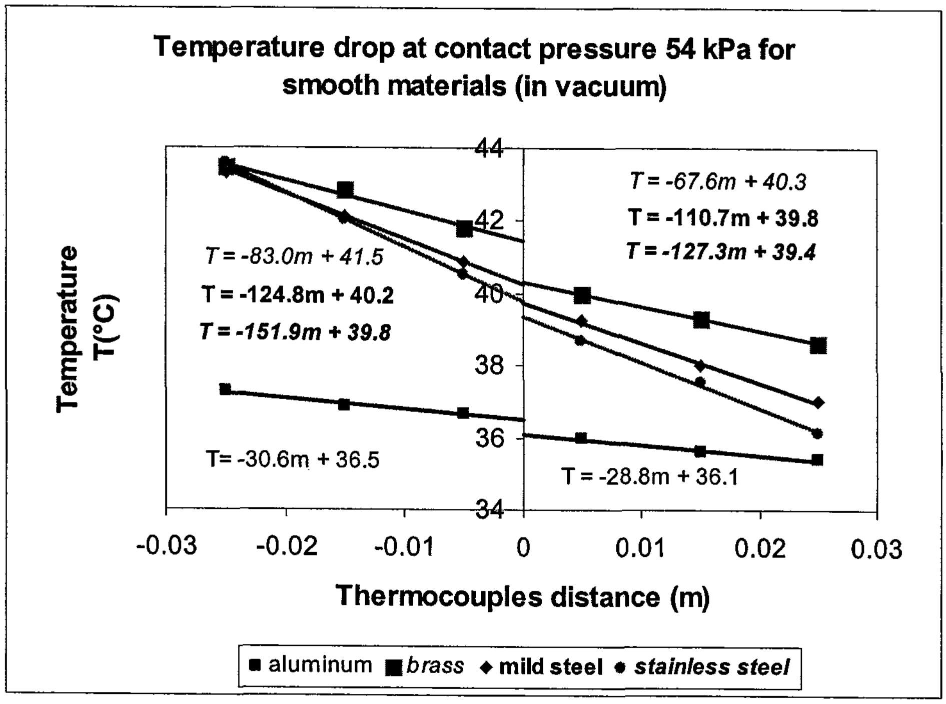

Figure 5.1 Temperature drop between specimen interfaces (smooth surfaces) in vacuum at contact pressure 54kPa.

In Figure 5.1, aluminum, brass and stainless steel have the same value of temperature drop of about 0.4°C and for mild steel is about 1.2°C. The data is taken for the contact pressure of 54kPa. The temperature gradients are used to calculate the heat flow for all the specimens for upper and lower specimens. Under contact pressure 54kPa, aluminum has the temperature gradient between -28.8 to -30.6, for brass is between -67.6 to -83, for mild steel is between -110.7 to -124.8 and for stainless steel is between -127.3 to -151.9. The temperature drop and the temperature gradient are then used to find the thermal contact resistance between interfaces.

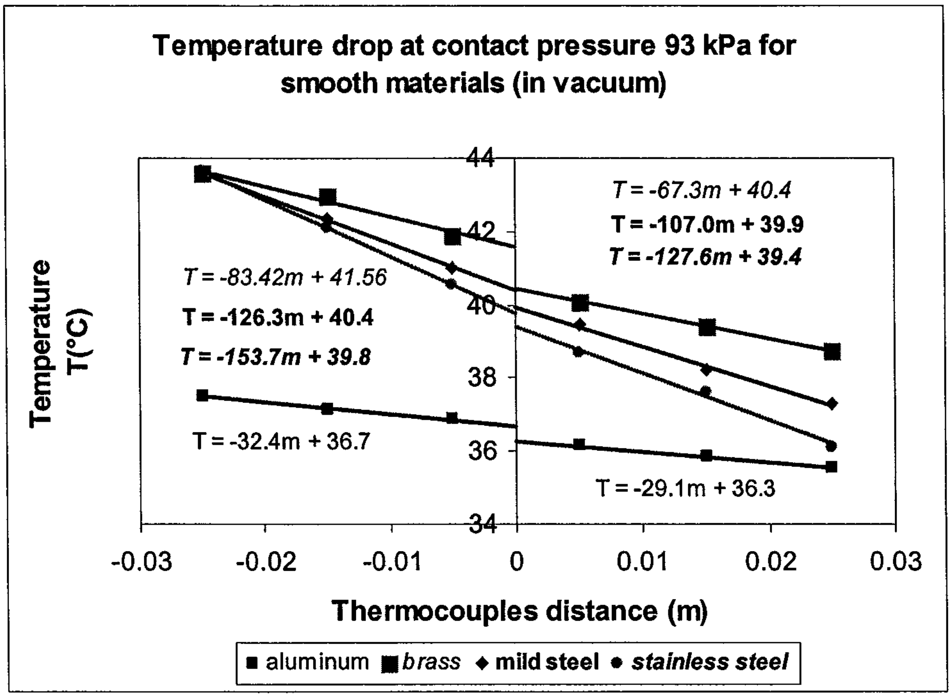

Figure 5.2 Temperature drop between specimen interfaces (smooth surfaces) in vacuum at contact pressure 93kPa.

In Figure 5.2, a similar value of temperature drop obtained as in Figure 5.1 (0.4°C) for aluminum and stainless steel. The temperature drops for mild steel and brass are 0.5°C and 1.16°C respectively. The temperature gradient for the contact pressure 93kPa is between -29.1 to -32.4 for aluminum, -67.3 to -83.4 for brass, -107 to -126.3 for mild steel and -127.6 to -153.7 for stainless steel.

The temperature drop at the ultimate contact pressure of 132kPa in vacuum for smooth surface specimens has been observed in Figure 5.3. For aluminum, the temperature drop is 0.3°C and stainless steel is 0.4°C. Mild steel and brass showed 0.4°C and 1.1°C temperature drop value. The temperature gradient for the contact pressure 132kPa is between -29.9 to -32.9 for aluminum, -67.3 to -83.2 for brass, -105.9 to -125.4 for mild steel and -130.8 to -

157.7 for stainless steel. From the temperature gradient obtained for the test conducted in vacuum with contact pressure up to 132kPa, the heat transfer rate can be said in steady state condition where the temperature gradient different between upper and lower specimen are small.

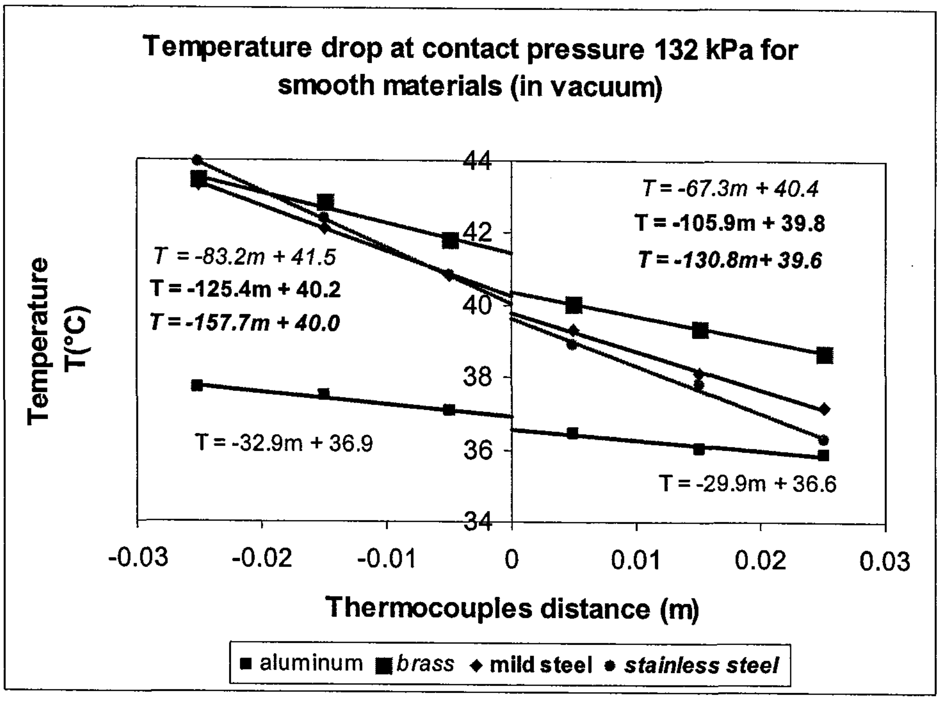

Figure 5.3 Temperature drop between specimen interfaces (smooth surfaces) in vacuum at contact pressure 132kPa.

For aluminum as the smoothest surfaces in vacuum condition test, the temperature drop value is very small. The same results obtained for the stainless steel. The relation between smooth surfaces with thermal contact resistance showed that the smoother the surfaces, the smaller the temperature drop value at the interfaces and thus producing good thermal conduction with low thermal contact resistance.

The temperature drop at the interface for smooth surface in ambient is also described in Figures 5.4, 5.5 and 5.6. The value is still smaller even though tested in different surrounding. For aluminum and brass, the temperature drop is about 1.3°C and 1.2°C for stainless steel (see Figure 5.4). The temperature gradient in ambient with contact pressure of 54kPa, is between -35 to -40 for aluminum, -75 to -90 for brass and -190 to -215 for stainless steel.

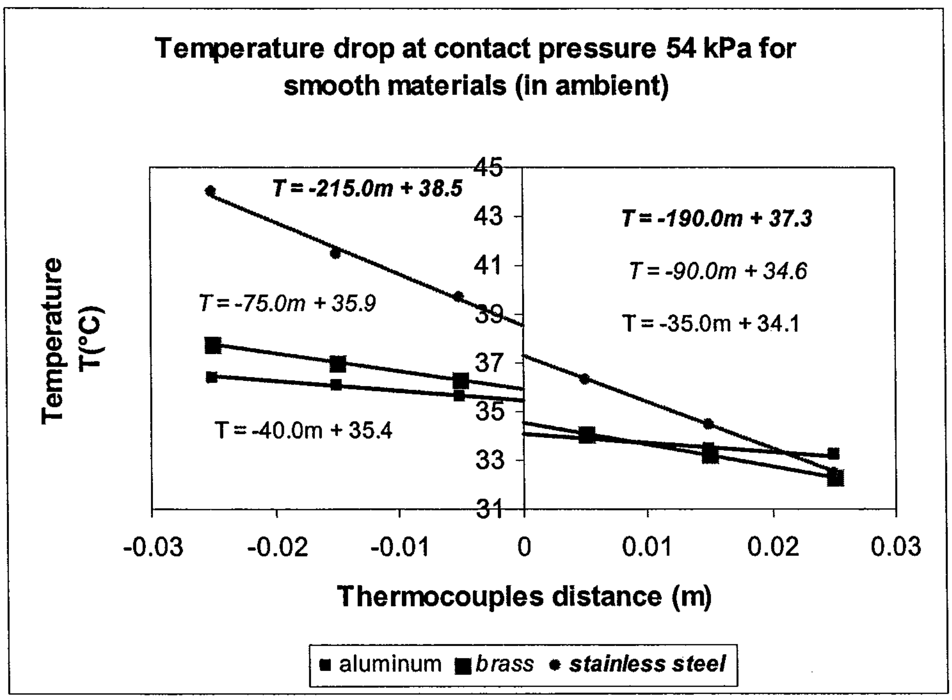

Figure 5.4 Temperature drops between specimen interfaces (smooth surfaces) in ambient at contact pressure 54kPa.

For the smooth surface in ambient with contact pressure of 93kPa (Figure 5.5), the temperature drop is about 1.2°C for aluminum and stainless steel when the contact pressure increased. Brass showed 1.3°C in temperature drop or the same value at 54kPa. The temperature gradient in ambient with contact pressure of 93kPa, is between -35 to -45 for aluminum, -75 to -80 for brass and -170 to -200 for stainless steel.

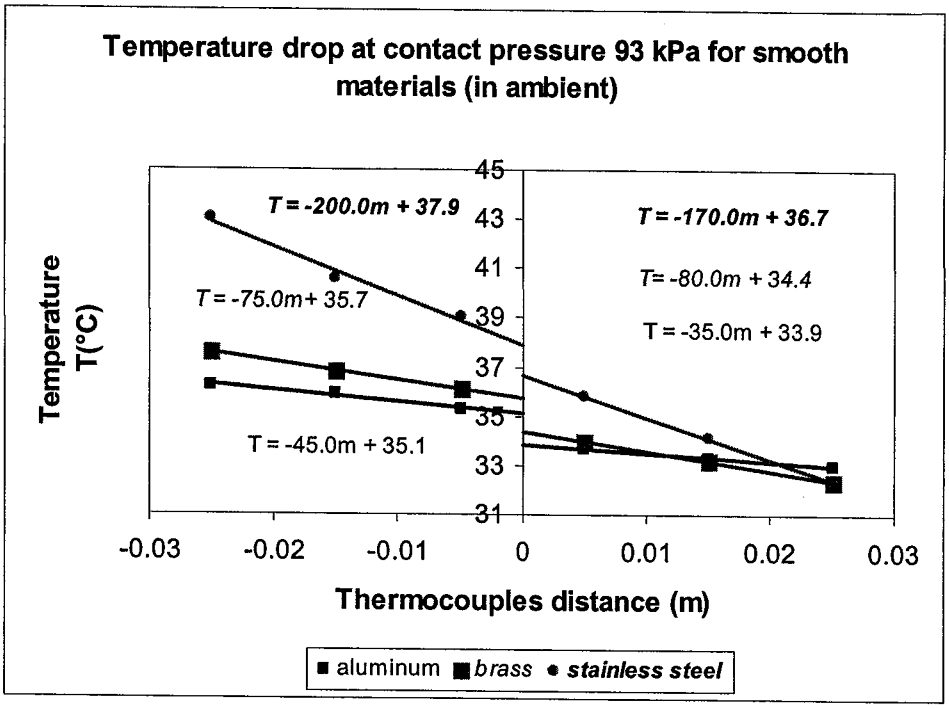

Figure 5.5 Temperature drop between specimen interfaces (smooth surfaces) in ambient at contact pressure 93kPa

Finally, the temperatures drop for smooth surface at the contact pressure of 132kPa in ambient have been shown in Figure 5.6. For aluminum and brass, the temperature drop is 1.1°C and for stainless steel is 0.9°C. The temperature gradient is -40 for aluminum, -75 to -85 for brass and -175 to -195 for stainless steel. The temperature gradient obtained showed that the heat transfer rates for all the specimens in ambient are in steady state condition.

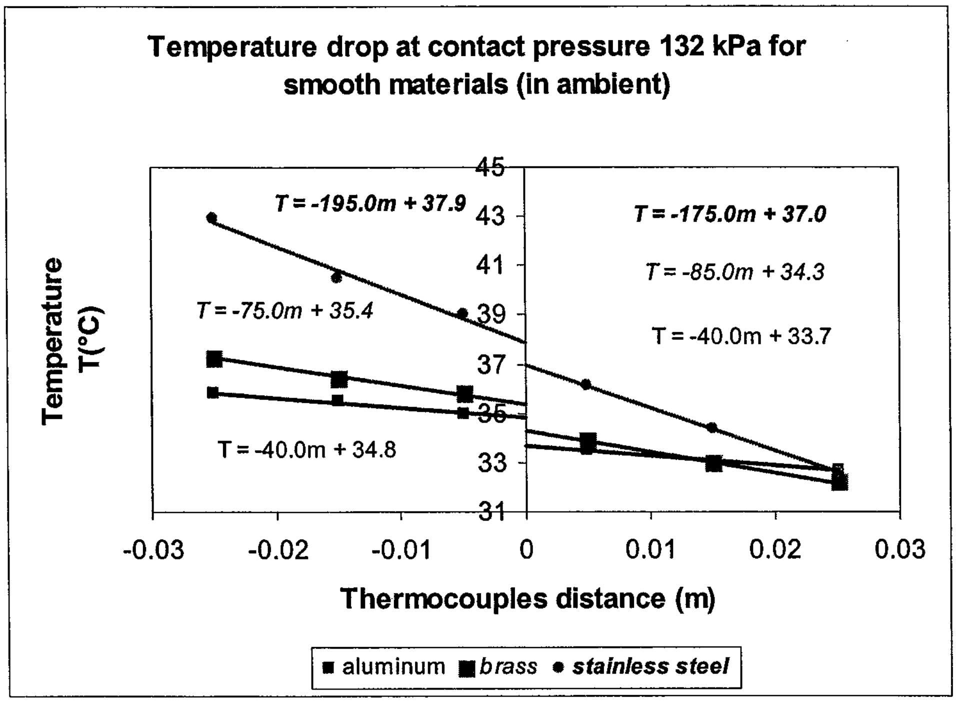

Figure 5.6 Temperature drops between specimen interfaces (smooth surfaces) in ambient at contact pressure 132kPa.

The temperature drop value is small and sometime constant with the contact pressure increases for all the smooth surfaces specimens in both conditions. Thus, the thermal contact resistance values for smooth surfaces are unchanged with low contact pressure. The small value of temperature drop provided small value of thermal contact resistance. The ultimate contact pressure of 132kPa has not given any significant change to the temperature drop.

5.1.2 Effect of rough surface to the temperature drop at the interfaces

Different results obtained in the temperature drop for rough surfaces in vacuum and ambient surrounding test. In Table 5.3, some of the surface roughness value for selected specimen has been given. In this table, the specimens surfaces roughness δ_1 and δ_2 approximately above 1.0 μm and assumed to be rough surfaces

Table 5.3 Specimens surface roughness (rough).

Spesimen	Specimens surface roughness (μm)					
	R_q (in vacuum)			R_q (in ambient)		
	δ_1	δ_2	δ	δ_1	δ_2	δ
aluminum	1.83	3.10	3.60	2.58	2.41	3.53
brass	2.60	2.83	3.84	-	-	-
mild steel	4.25	2.75	5.06	2.68	3.62	4.50
stainless steel	2.35	3.18	3.95	3.31	3.62	4.91

For the rough surface in vacuum with contact pressure of 54kPa as indicated in Figure 5.7, the temperature drop for aluminum is about 1.4°C, for brass is 2.3°C, for mild steel is 5.6°C and stainless steel is 1.7°C. For all the specimens, the value of the temperature drop is greater than the value for the same specimens with smooth surfaces. They are shown that the higher value of roughness will give higher temperature drop. The same phenomena can be observed in Figure 5.8 and 5.9.

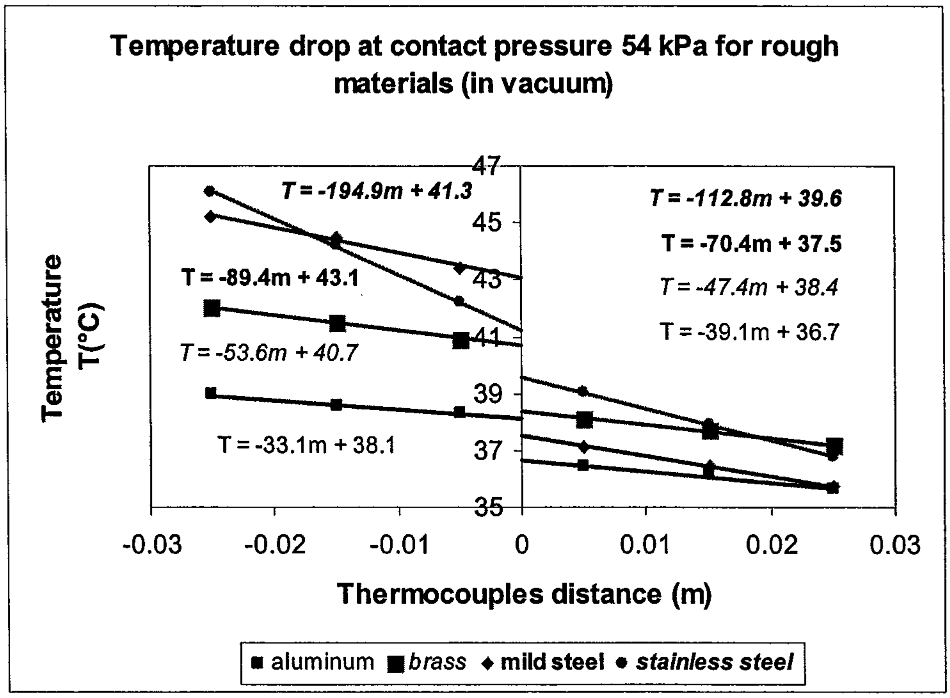

Figure 5.7 Temperature drop between specimen interfaces (rough surfaces) in vacuum at contact pressure 54kPa.

The temperature gradient for rough surfaces in vacuum under contact pressure 54kPa is between -33.1 to -39.1 for aluminum, -47.4 to -53.6 for brass, -70.4 to -89.4 for mild steel and -112.8 to -194.9 for stainless steel.

For the contact pressure of 93kPa as indicated in Figure 5.9, the temperature drop for aluminum is about 1.4°C, for brass is 2.2°C, for mild steel is 5.5°C and stainless steel is 1.7°C respectively. These values are almost same with the result under contact pressure 54kPa. The temperature gradient also almost similar which is between -34.5 to -39.2 for aluminum, -47.5 to -53.2 for brass, -70.7 to -89.8 for mild steel and -112.8 to -194.9 for stainless steel.

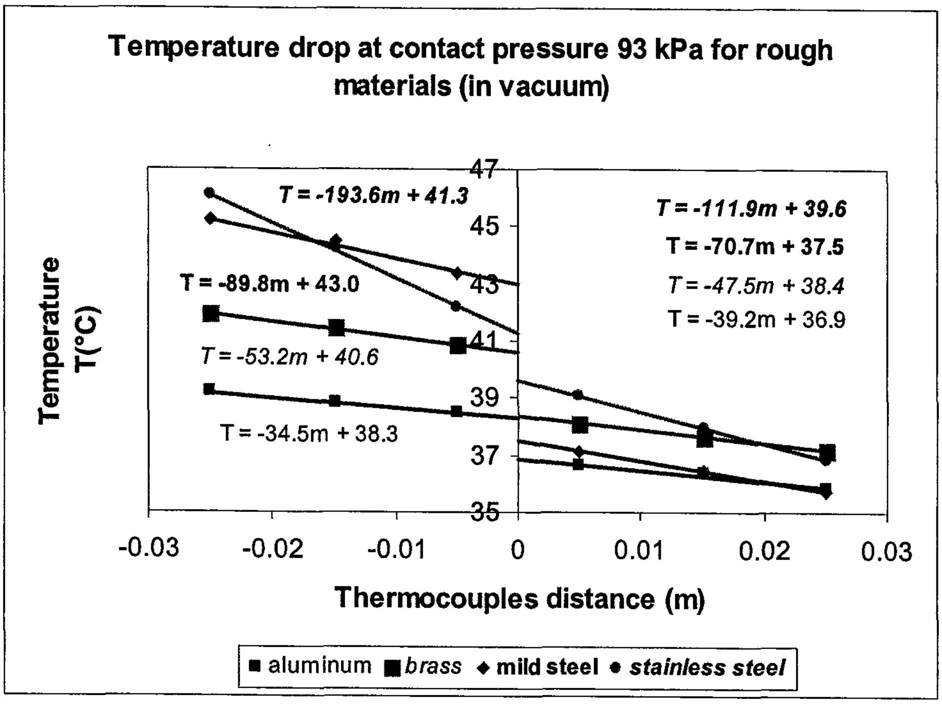

Figure 5.8 Temperature drop between specimen interfaces (rough surfaces) in vacuum at contact pressure 93kPa.

When the highest contact pressure of 132kPa applied to the rough specimens, (Figure 5.10) similar trend of the results are shown as in Figure 5.8 and 5.9. The temperature drop value for aluminum is 1.5°C, brass is 2.3°C, mild steel is 5.3°C and stainless steel is 1.7°C. The temperature drop for mild steel showed the highest value as this specimen has the roughest surface compared with other specimens as indicated in Table 5.3.

The temperature gradient is between -35.8 to -41.9 for aluminum, -49.8 to -55.6 for brass, -68.5 to -89.5 for mild steel and -111.1 to -192.7 for stainless steel. From the results, the temperature gradient do not much influenced on the heat flow through the surfaces. Therefore, the heat transfer through upper and lower specimens is said to be in steady state condition.

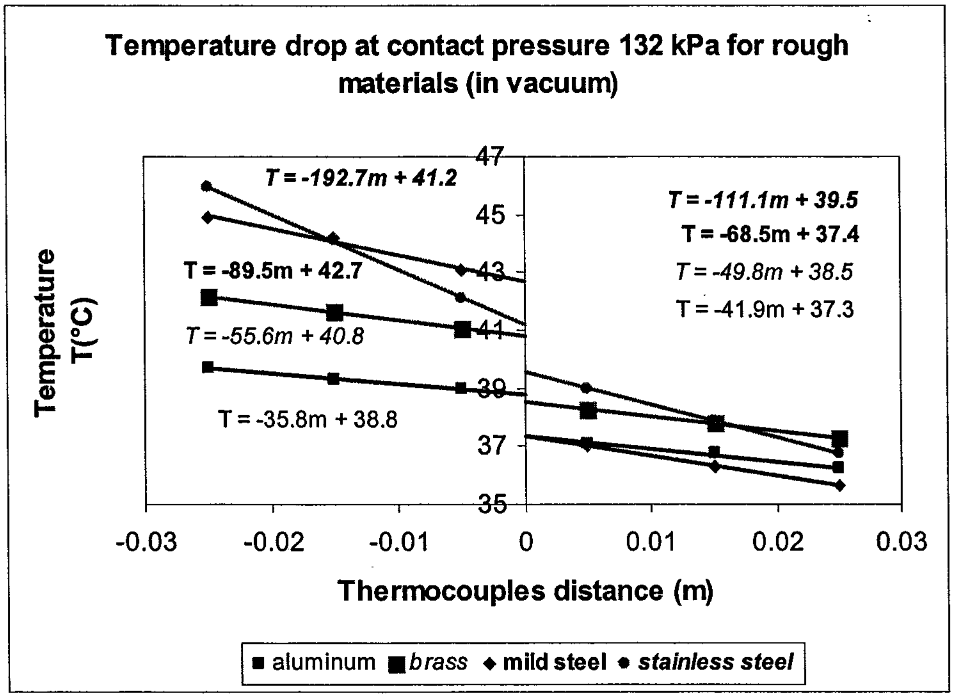

Figure 5.9 Temperature drops between specimen interfaces (rough surfaces) in vacuum at contact pressure 132kPa.

These phenomena again had given the conclusion about the surface topography of any materials in contact when heat is flow between these surfaces in steady state condition. By measuring the surface roughness of the contact area, estimation on the thermal contact resistance can be made. The results show that the higher the surface roughness, the higher the thermal contact resistance.

The effect of surface roughness has been repeated in different environment i.e. vacuum and atmospheric or ambient conditions; for both smooth and rough specimens. In Figures 5.10, 5.11 and 5.12, the test for rough mating surfaces have been made in ambient condition. As in Figure 5.10, the temperature drop for aluminum, mild steel and stainless steel have been revealed. The temperature drop value for aluminum is 7.7°C, mild steel is 7.3°C and stainless steel is 5.1°C.

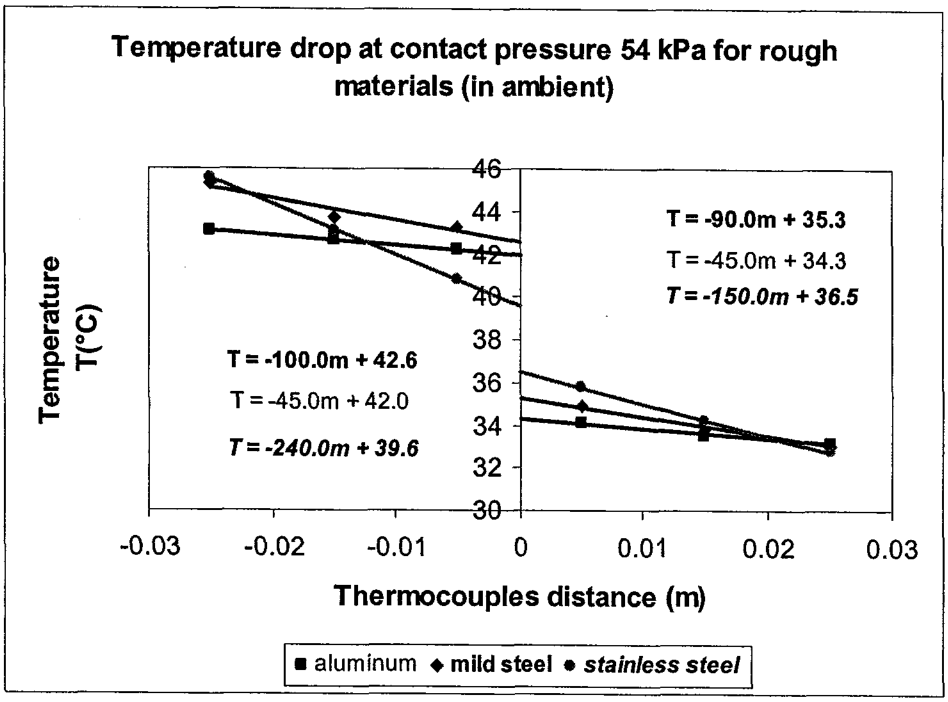

Figure 5.10 Temperature drops between specimen interfaces (rough surfaces) in ambient at contact pressure 54kPa.

The temperature gradient is -45 for aluminum, -90 to -100 for mild steel and -150 to -240 for stainless steel (Figure 5.10).

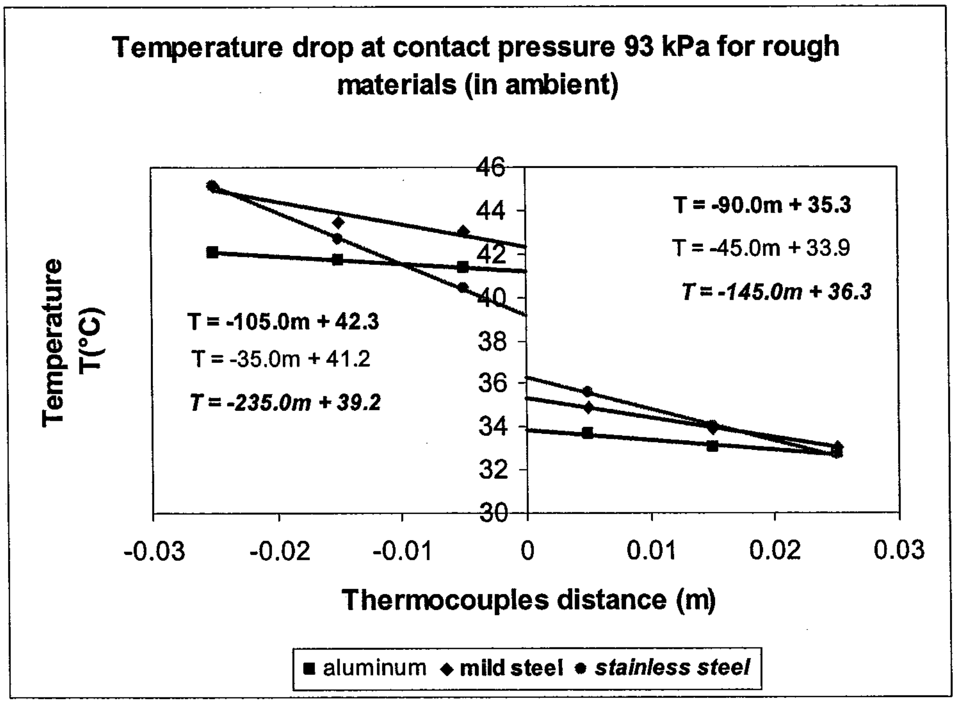

Figure 5.11 Temperature drops between specimen interfaces (rough surfaces) in ambient at contact pressure 93kPa.

In Figure 5.11, the temperature drop value for aluminum is 7.3°C, mild steel is 7°C and stainless steel is 2.9°C. The temperature drop for all specimen decrease with the contact pressure increases. The temperature drops reduce due to the air trapped between the interstitial gaps in ambient surrounding have moved out from the interfaces and thus reducing the thermal contact resistance. The temperature gradient for the specimens is -35 to -45 for aluminum, -90 to -105 for mild steel and -145 to -235 for stainless steel (Figure 5.11).

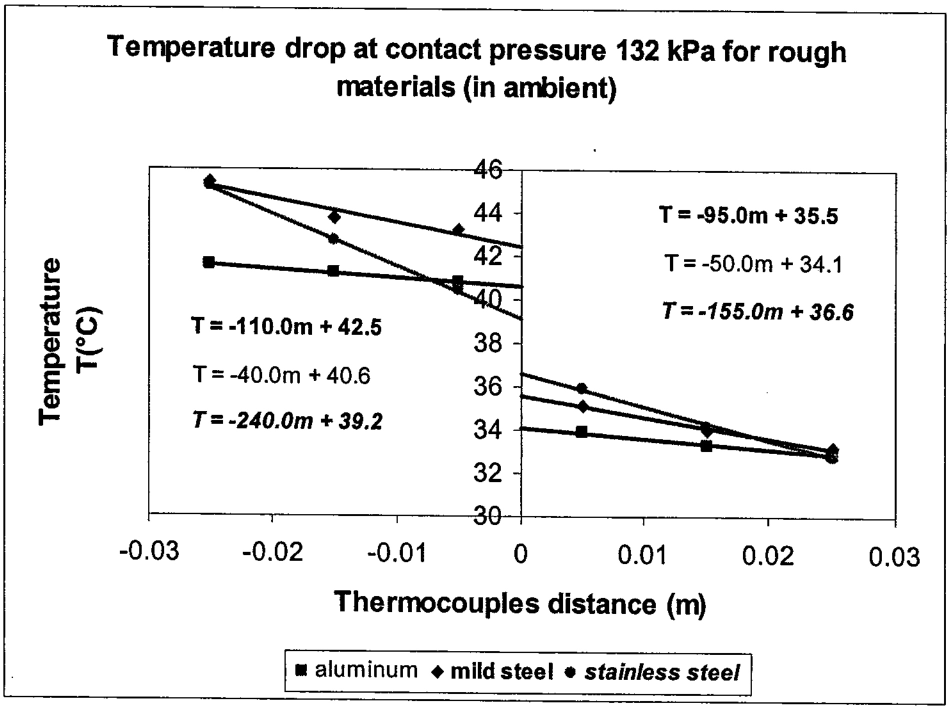

Figure 5.12 Temperature drops between specimen interfaces (rough surfaces) in ambient at contact pressure 132kPa.

Finally in Figure 5.12, the temperature drop value for aluminum is 6.5°C, mild steel is 7°C and stainless steel is 2.6°C. The temperature drop for aluminum and stainless steel reduce as expected while the results for mild steel remain constant. For rough surfaces either in vacuum and ambient condition, the temperature drop is higher compared to the smooth surfaces. Except for stainless steel which have big different in temperature gradient between upper and lower specimens with -155 to -240, the temperature gradient for aluminum and mild steel is still small between -40 to -50 and -95 to -110 respectively. The heat transfer can be assumed in steady state condition during the experimental test for rough surfaces in ambient environment.

In overall, the value of surface roughness plays an important role to determine the results of thermal contact resistance. The surface roughness of specimens has provided significant effects on the temperature drop at interfaces and thermal contact resistance.

5.2 Effect of the contact pressure to the thermal contact resistance

Another important factor that determined the thermal contact resistance (TCR) value is the effect of contact pressure. It is shown in Table 5.4 and Table 5.5. Aluminum has the highest of TCR decreased percentage for both vacuum and ambient condition. Aluminum and stainless steel are categorized as softest and hardest materials respectively.

Table 5.4 The effect of contact pressure in vacuum environment

contact pressure (kPa)	Thermal contact resistance value (°C/W)			
	Aluminum	Brass	mild steel	stainless steel
34.82	0.398	0.334	2.844	1.433
54.16	0.386	0.331	2.819	1.416
73.51	0.385	0.332	2.811	1.417
92.85	0.380	0.326	2.795	1.422
112.19	0.376	0.328	2.835	1.396
131.54	0.373	0.329	2.750	1.396
TCR decreased	6.3%	1.5%	3.3%	2.6%

In Table 5.4, Aluminum has the highest of thermal contact resistance reduced as much as 6.3% for the contact pressure between 34kPa to 132kPa. It's followed by stainless steel, mild steel and brass. The softest mating material particularly aluminum, TCR gradually reduced up to 0.025°C/W at the contact pressure of 132kPa. It is belief that the contact pressure has changed the surface deformation of the aluminum asperity. The elastic deformation may be occurred during this stage. Higher contact pressure may increase the contact surface area.

Table 5.5 The effect of contact pressure in ambient environment

contact pressure (kPa)	Thermal contact resistance value (°C/W)			
	aluminum	brass	mild steel	stainless steel
34.82	2.194	0.141	3.132	2.078
54.16	2.009	0.163	3.132	2.043
73.51	1.990	0.134	3.047	1.747
92.85	1.797	0.139	2.909	2.016
112.19	1.559	0.139	2.784	1.703
131.54	1.490	0.134	2.748	1.681
TCR decreased	32.1%	5.0%	12.3%	19.1%

In ambient environment, Table 5.5 illustrates the TCR. Again, the results show that TCR reduces about 32.1% for aluminum followed by stainless steel, mild steel and brass with 19%, 12% and 5% respectively. Thus, Aluminum has shown the highest percentage of thermal contact resistance (TCR) decreases for both vacuum and ambient environment. In ambient environment, it is found that the decreased of TCR for aluminum gradually reduced up to 0.704°C/W at the contact pressure of 132kPa. The contact pressure again has changed the surface deformation of the aluminum asperity.

5.3 Effect of the material hardness on the thermal contact resistance

The surface microhardness value is another significant factor affecting the thermal contact resistance. The results for aluminum and brass are almost same trend. Instead of the high thermal conductivity value k (W/mK) for both specimens such as aluminum and brass, it is found that the TCR values also influenced by the hardness of these materials. Brass surface is harder (1441H_v) than aluminum (470.7H_v), but almost equal to mild steel (1541H_v). The stainless steel is the hardest material with (2795H_v). H_v is the Vickers microhardness measurement units in MPa and the values (see Table 5.6) obtained from the measurement by using Mitutoyo Vickers Microhardness. Aluminum is the softest material followed by brass, while stainless steel is the hardest material followed by mild steel. The TCR values also increased with the increasing of the hardness of the materials as shown in Table 5.7. Aluminum has the lowest TCR value, followed by brass, mild steel and stainless steel respectively. This indicated that aluminum has experienced the surface plastic deformation under the low applied contact pressure (34kPa – 132kPa). Other materials such as brass, mild steel and stainless steel may experience elastoplastic deformation during the experiment.

Four different types of specimen materials have been chose based on the hardness of the materials. The hardness of the materials always became the important factor in most theoretical models. The materials used were aluminum, brass, mild steel and stainless steel.

Table 5.6 The different of specimen's hardness value

Specimen material			
aluminum	brass	mild steel	stainless steel
Vickers microhardness value, H_v (MPa)			
471	1441	1541	2795

The hardness of all the specimens has been measured from Mitutoyo Vickers microhardness unit. This value used to predict the TCR value using the theoretical model for aluminum discussed at the end of this chapter.

Table 5.7 The TCR values for different hardness materials

Thermal contact resistance range (°C/W)			
aluminum	brass	mild steel	stainless steel
(0.112 - 0.127)	(0.126 - 0.131)	(0.151 - 0.180)	(0.353 - 0.366)

Figure 5.13 indicated the thermal contact resistance for the mating surfaces of aluminum, brass, mild steel and stainless steel with smooth surfaces in vacuum condition. Aluminum showed the lowest thermal contact resistance value while stainless steel produced the highest. The thermal contact resistance values are given in Table 5.7.

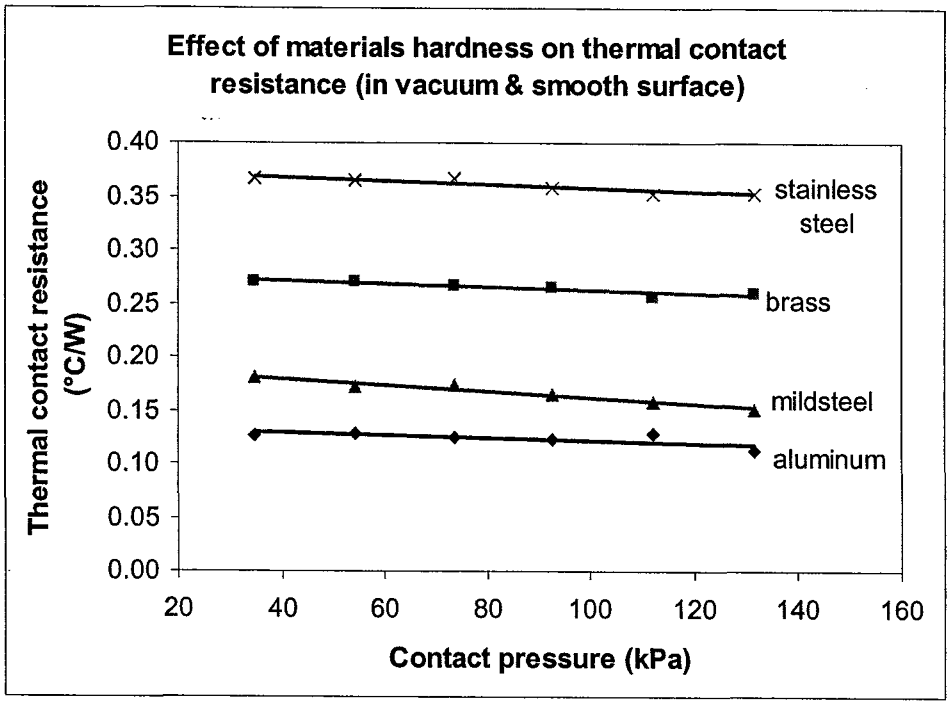

Figure 5.13 Thermal contact resistance graph for different hardness

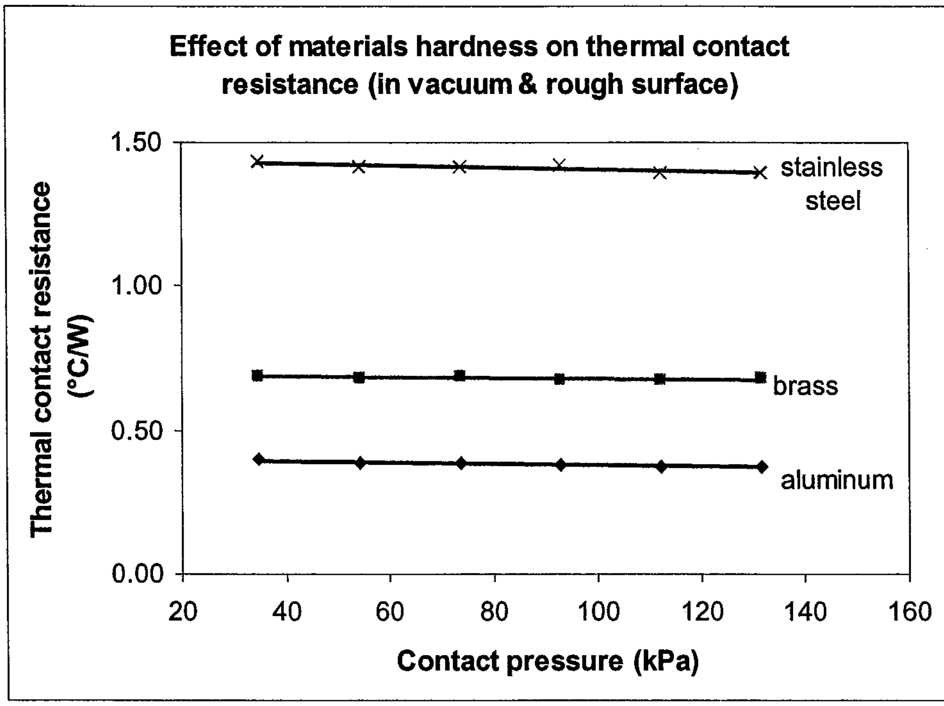

Figure 5.14 Thermal contact resistance graph for different hardness

Figures 5.13 and 5.14 showed the effect of material hardness for different specimens in both environments. It is found that Aluminum remains as the lowest value of thermal contact resistance followed by brass and stainless steel (Figure 5.14). For both results in Figures 5.13 and 5.14, the material thermal and mechanical behavior described their thermal contact resistance. The softer the material, the better the TCR and the harder material produced higher TCR. The microcontact which occurred between upper and lower surfaces asperities is influenced by the microhardness. The elastic and plastic deformation of the asperity slopes also referred to the surface microhardness as discussed in the literature reviews. Thus became the major factor for aluminum to produce better results compared with other specimens.

5.4 Results Comparison and Discussion.

From the results obtained, there are many factors that influenced the value of contact thermal resistance. Some are obviously can be mentioned such as the contact surface topography which has been validated through this experiment. The results for both smooth and rough surfaces has a big different as expected. The value of the temperature drop is smaller for smooth surface rather then rough surface under the same increasing in contact pressure. The reason for this is the smoother the surfaces, the higher the actual contact area and the lower the height of the asperity slopes. This gave the lower thermal contact resistance value compared with rough surfaces. It can be clearly observed in Table 5.1 where the value of thermal contact resistance for the same materials with different surfaces is given. Rough surface will definitely produce bad contact rather than smooth surface.

However, for different material with surface type within the range of determined surface roughness, the proper contact will be based on other parameter such as the hardness of the material, the applied contact pressure and the interstitial fluid or gases trapped between gaps. The material property such as elasticity of the material also needs to be considered. When the pressure applied on the contact spot released, the elasticity of the material will caused the contact spot remain to it actual condition or surface structure. This can affect the thermal contact resistance. However, the elasticity would no longer affect the contact after the pressure applied exceeding the maximum value that makes the specimens surface grains lost their elastic and get into fully plastic state. This has been mentioned clearly by Greenwood and Tripp (1970). The different test environment also showed significant effect as discussed in 5.4.1 while the comparison between experimental and theoretical results are discussed in 5.4.2.

5.4.1 Comparison between ambient and vacuum condition

The experiments have been made in two different environments which are in ambient and in vacuum environment. Significant differences in TCR can be seen from the results obtained from both condition. The results obtained from vacuum environment are lower than in ambient environment for all specimens. Many cases involving the TCR between mechanical joints or contact surfaces occurred in ambient environment under atmospheric pressure.

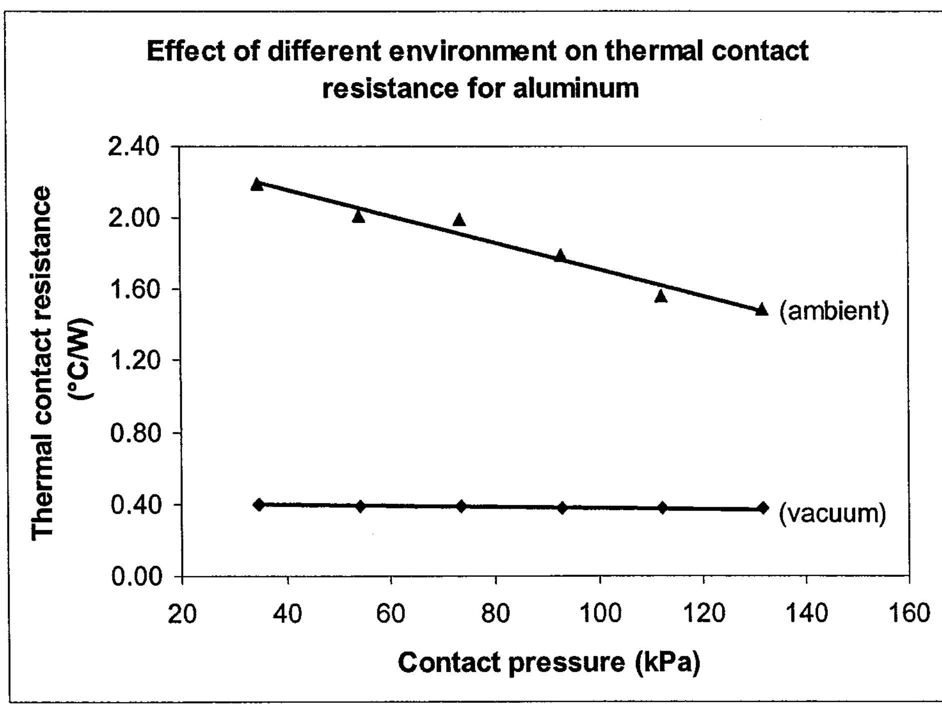

Figure 5.15 Thermal contact resistance graph for Aluminum in different environment

The results for different environment become important to the theoretical models considered for both environments. Figure 5.15 indicated the thermal contact resistance for aluminum in different environment. Instead of higher thermal contact resistance value, the results for ambient condition also gave scatter data rather then in vacuum condition. The existence of air that trapped between the interstitial gaps of contacting surfaces may be contributed to this situation. The same trend obtained for mild steel and stainless steel such as in Figure 5.16 and 5.17.

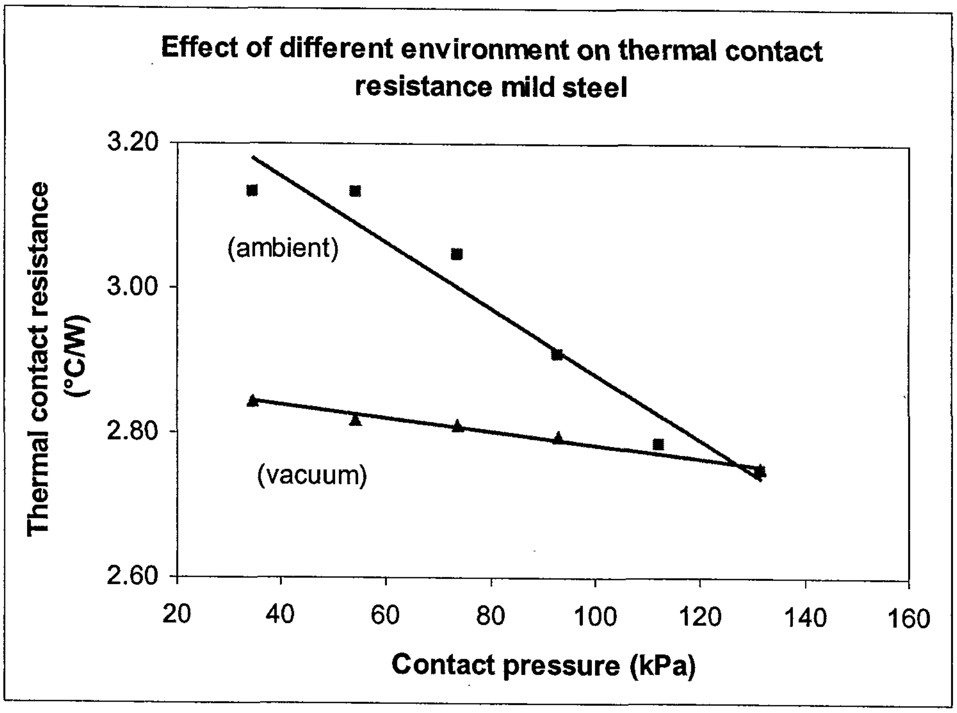

Figure 5.16 Thermal contact resistance graph for mild steel in different environment

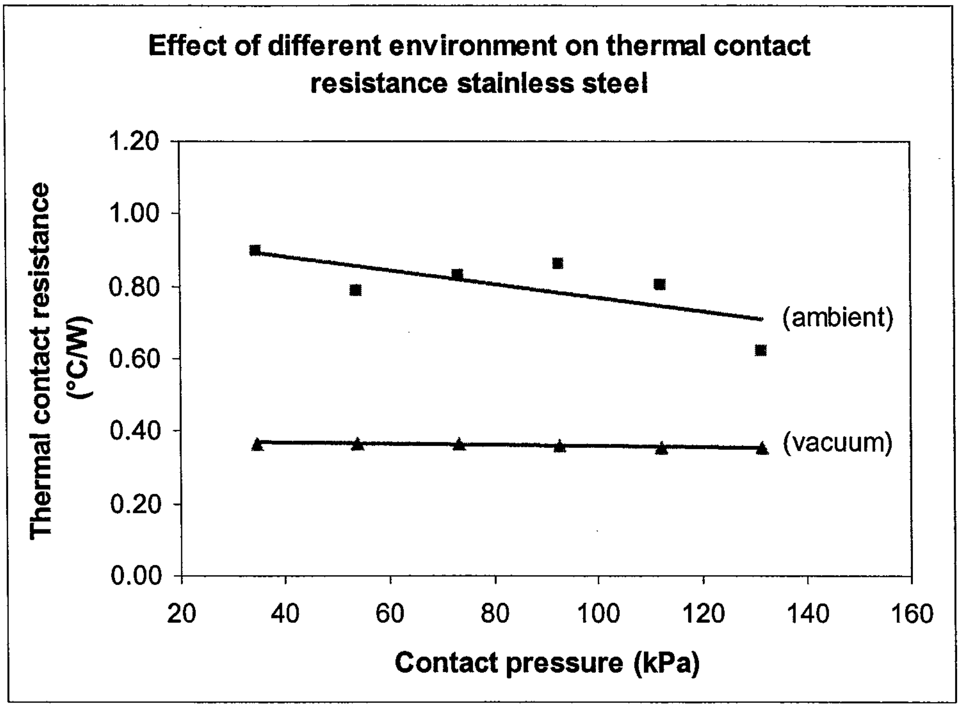

Figure 5.17 Thermal contact resistance graph for stainless steel in different environment

For the comparison results on different environment, all the data obtained in vacuum is said to be better than in ambient environment. Even though for the specimens used in the experimental test in vacuum is not being insulated, the convection can be neglected and the radiation may not gave the significant effect if the material temperature is lower than 300°C (Wahid and Madhusudana, 2000). The test surrounding can be varied according to the any cases which involved the thermal contact resistance problem. For most of electronic products such as the silicon chips where aluminum heat sink is used to remove the heat from the chip, the preferred surrounding condition is in ambient environment. However, for the cases of aerospace equipment such as satellite, vacuum condition will be better. For theoretical prediction, most of the thermal conduction models separate the calculation on the effect of interstitial gases with the calculation of actual contact area. These values can be combined if ambient condition is considered.

5.5 Comparison between experimental and prediction

Comparison between experimental result and theoretical models also has been made. Theoretical prediction has been done on aluminum by using the Model proposed by Cooper, Mikic and Yovanovich (CMY).

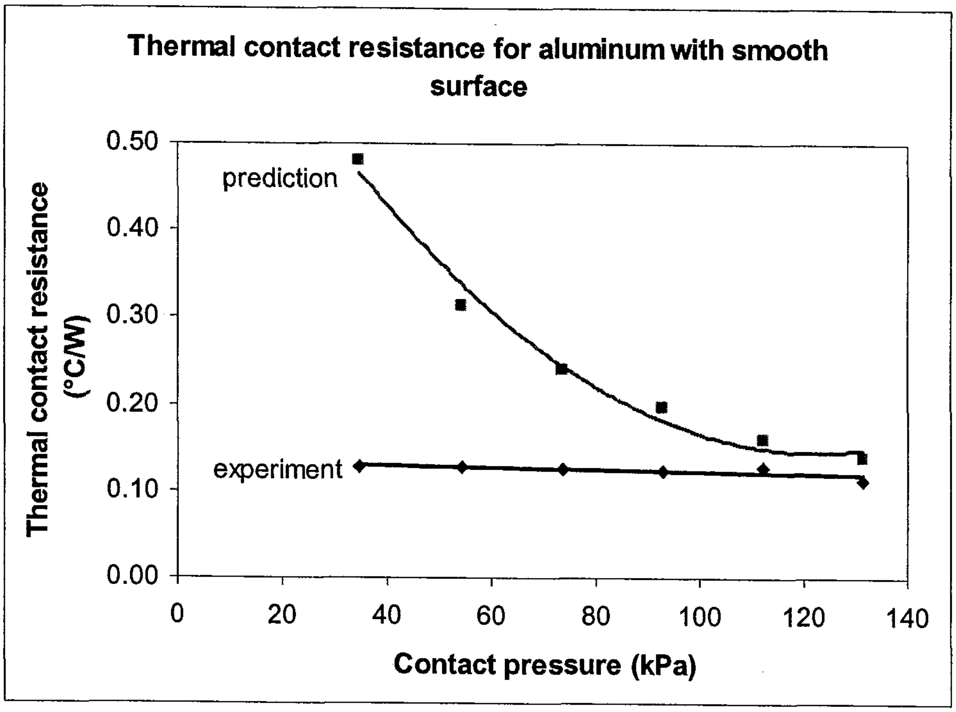

Figure 5.18 The comparison between experiment and CMY Model prediction value for aluminum with smooth surface

It is shown in Figures 5.18 and 5.19 that the CMY model predicted better for aluminum then other materials. The reason for these might be because of the low contact pressure and the materials mechanical properties which referred to the hardness and surface roughness. Figures 5.20 and 5.21 showed the prediction results on brass and mild steel using CMY Model. The prediction is not very well compared with aluminum specimens.

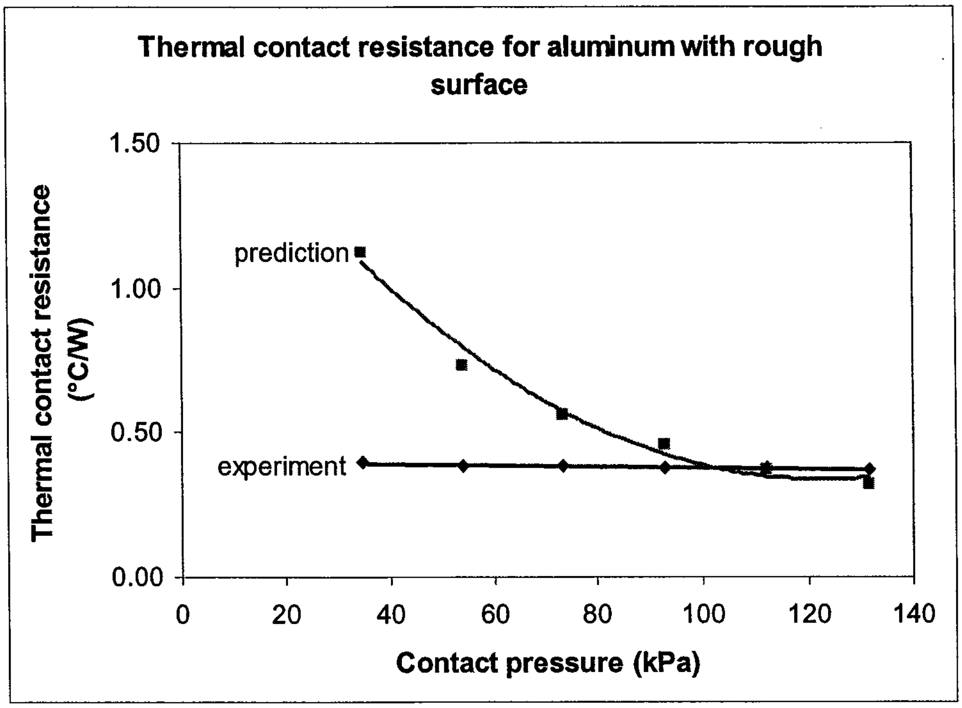

Figure 5.19 The comparison between experiment and CMY Model prediction value for aluminum with rough surface.

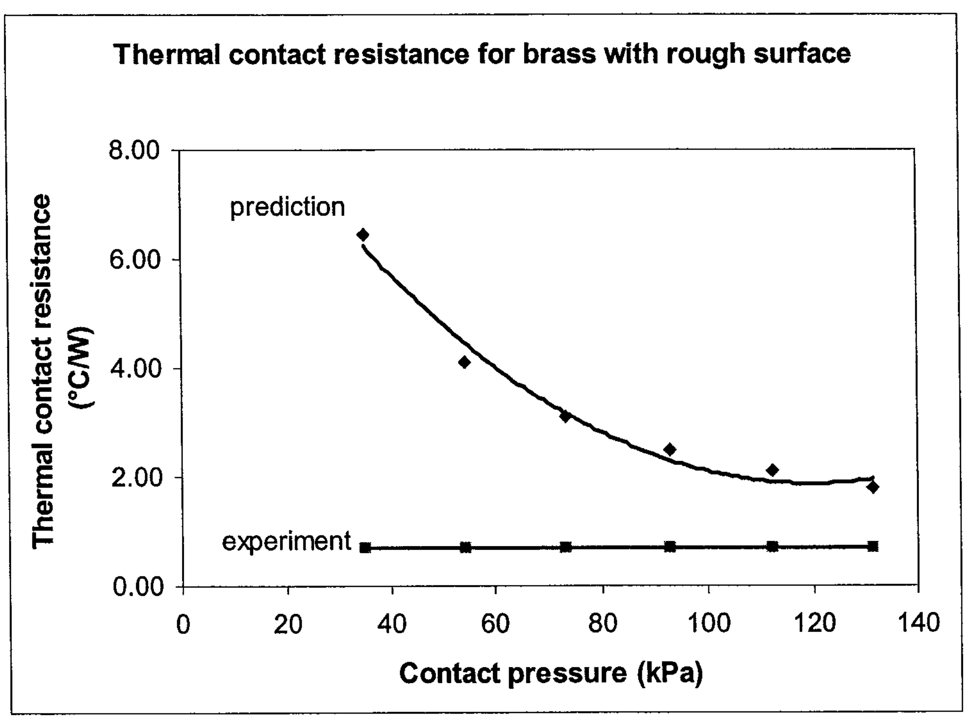

Figure 5.20 The comparison between experiment and CMY Model prediction value for brass with rough surface

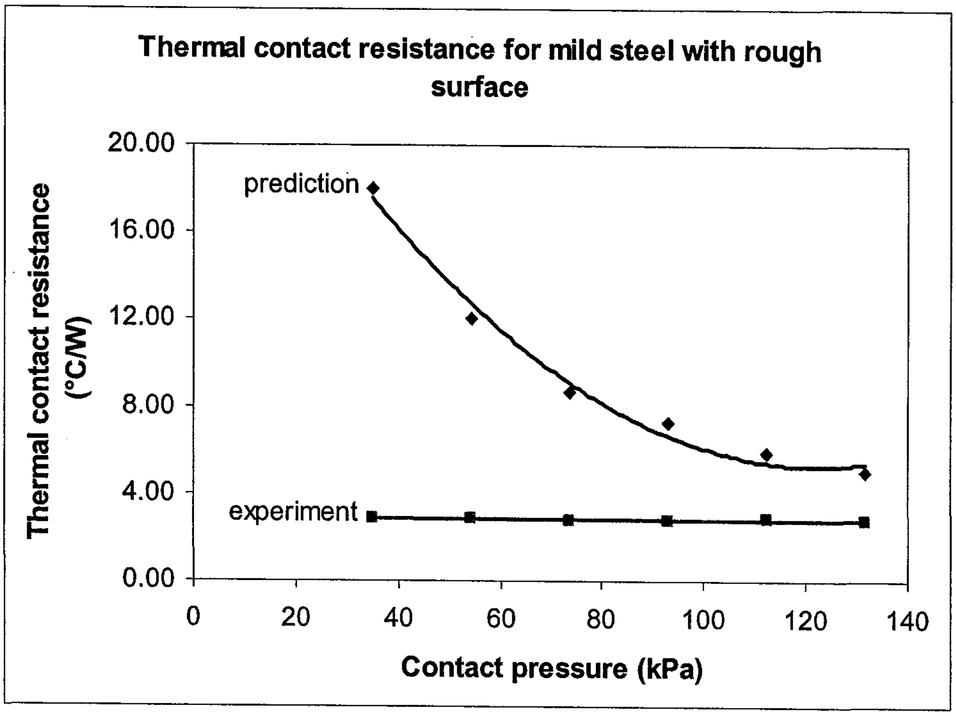

Figure 5.21 The comparison between experiment and CMY Model prediction value for mild steel with rough surface

Aluminum that is said to be the softest material with smooth surface showed better prediction results compared with the aluminum with rough surfaces. For aluminum with both smooth and rough surface, the agreement of TCR value can be found within the contact pressure between 73.51 KPa to 92.85 KPa. This can be observed in Figure 5.7 and Figure 5.8. Thus, it can be said that the CMY Model predicted better when the contact pressure is increased. Furthermore, the aluminum surface asperity experienced more plastic deformation rather than brass, mild steel and stainless steel. The prediction for brass and mild steel must also consider on the elastic deformation. This is the reason for choosing the Plastic CMY Model to predict the thermal contact resistance value of aluminum specimens such as discussed in Chapter 4.

As the aluminum thermal contact resistance value can be calculated approximately by the Plastic CMY Model, the real contact area also can be estimated. The estimated real contact area was based on the CMY model. The relative real contact area value is shown in Table 5.8.

Table 5.8 The values of estimation real contact area for aluminum (rough surface).

Contact pressure (KPa)	Apparent contact area A_a (mm^2)	ε^2	Real contact area A_r (mm^2)
34.82	507	0.00015	0.07
54.16	507	0.00023	0.12
73.51	507	0.00031	0.16
92.85	507	0.00039	0.20
112.19	507	0.00048	0.24
131.54	507	0.00056	0.28

5.4 Thermal contact resistance in Li-ion cell battery.

The experiment continued on the first electrode in the battery that was anode. The test on anode sandwiched between the upper and lower brass portion show high thermal contact resistance value which is from 1.609°C/W to 1.093°C/W. The TCR for cathode was higher which was in the range of 4.433°C/W to 4.260°C /W. The detailed results for cathode, anode and separator are given in Table 5.9 and plotted into the graph as shown in Figures 5.22 and 5.23.

Table 5.9 The TCR values for Li-ion cell electrode stack layer

Contact pressure (KPa)	Thermal contact resistance value (°C/W)				
	anode	cathode	separator	combined	Rengasamy & Ravigururajan (2004)
34.82	1.609	4.433	2.014	-	-
54.16	1.571	4.322	1.972	5.417	-
73.51	1.614	4.338	1.939	5.312	-
92.85	1.466	4.335	1.822	5.384	-
112.19	1.459	4.297	1.765	5.340	-
131.54	1.093	4.260	1.801	5.150	(5.52 – 6.7)

The thermal contact resistance value for Li-ion cell battery can be obtained by using experimental test. The theoretical prediction showed very much different value of thermal contact resistance compared to the experimental result. The rough surfaces of anode and cathode produced high thermal contact resistance value while the low thermal conductivity of polyethylene/polypropylene (PEPP) was probably the reason for high thermal contact resistance value for separator. For separator, the result showed that the thermal resistance obtained from the experiment was between 2.014°C/W to 1.801°C/W.

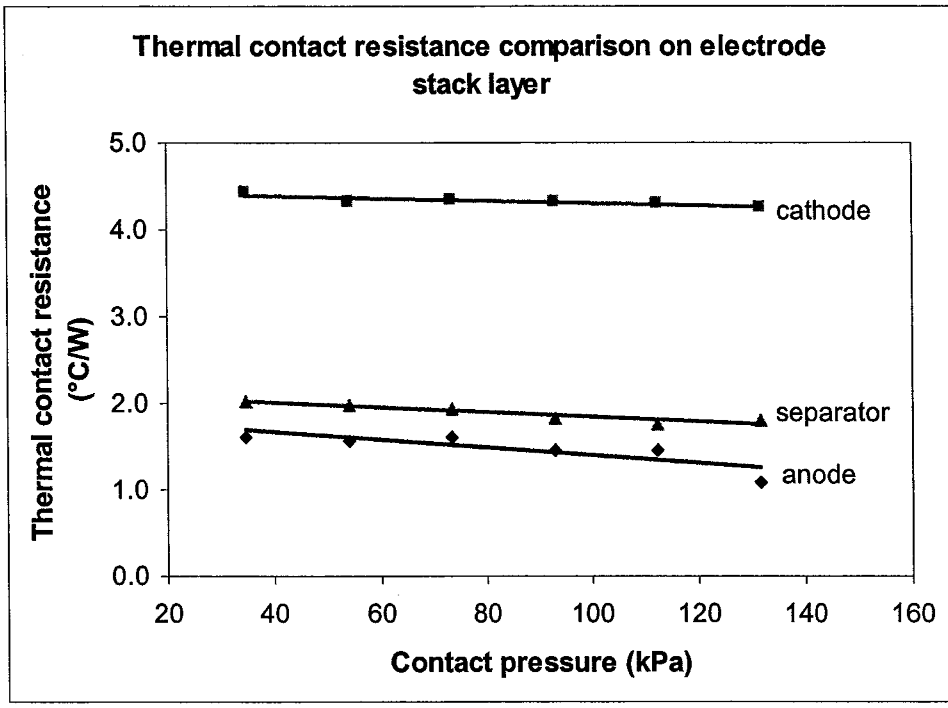

Figure 5.22 Thermal contact resistance graph for Li-ion battery electrode layers.

All the battery parts that consist of anode, separator and cathode were arranged by layer similar to the original layer in the battery pack and have been tested to get the thermal contact resistance with the result shown in Figure 5.23. The TCR value was 5.4 °C/W and decreased to about 5.2 °C/W when applying contact pressure. This result trend was similar to the result obtained by Rengasamy and Ravigururajan (2004), where the value for combined layers in their study were about 5.52 to 6.7 °C/W at 132kPa.

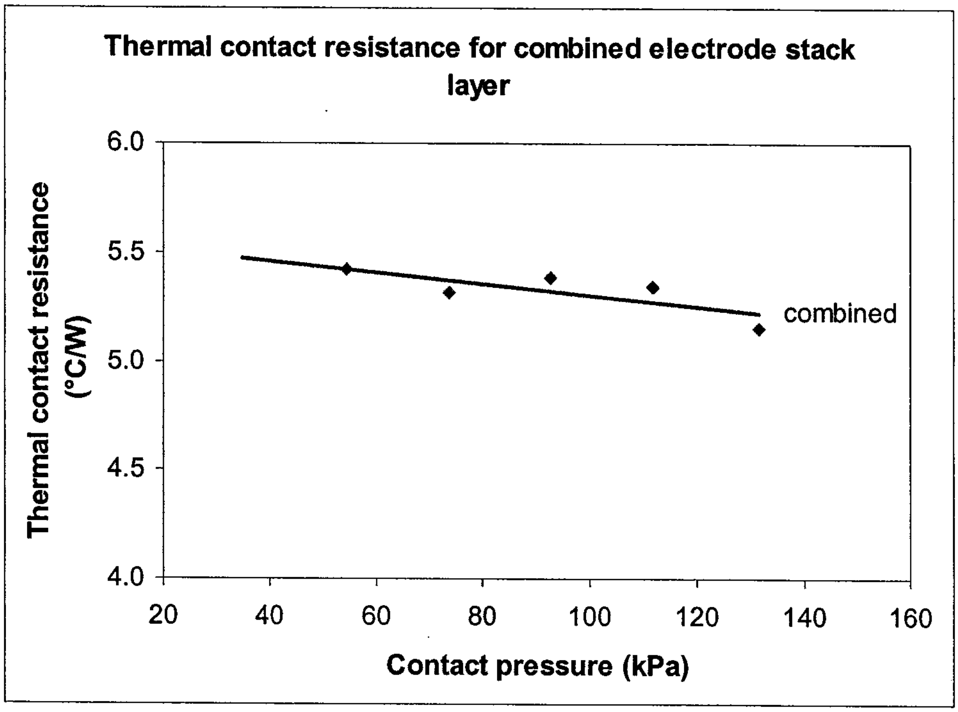

Figure 5.23 Thermal contact resistance graph for Li-ion battery with combined electrode layers

Some parameter in the theoretical calculation should be revised and measured such as hardness for coated and uncoated surfaces of the electrode layers so that the theoretical prediction can be used appropriately. The thermal contact resistance reduced significantly by increasing the contact pressure to the contact surfaces of the Li-ion cell electrode stack layers, (0-132KPa).

type and hardness of the materials, surface roughness and contact pressure have been recognized from the experimental investigation and verified according to the results.

6.1.2 Future works

Some suggestion regarding to this research have been proposed as mentioned below.

- Thermal Contact Resistance Model must be developed according to previous models produced in many literatures.
- Electronic or microelectronic components can be tested in the rig made in this research. However, the method to mount the components in the test section has to improve.
- The rig can be improved in certain parts such as the load applied method by using pneumatic or hydraulic pressure system so that the contact pressure can be measured properly. The cooling systems efficiency also can be improved by using a coolant to reduce the water temperature.
- An actual value of heat generated in any component must be obtained before testing in the rig.
- The thermal contact resistance model can be displayed in three dimensional numerical method to show the heat flow situation that occur at the interfaces during thermal contact for example the constriction and spreading thermal resistance.
- The surface topography of the surface in contact must be estimated according to the type of contact so that the real contact area can be easily modeled.

REFERENCES

Books:

Incropera, Frank P and DeWitt, David.P, (2002). *Introduction to Heat Transfer.* New York; John Wiley & Sons, USA.

Kraus, Allan D., Avram Bar-Cohen (1983), *Thermal Analysis and Control of Electronic equipment.* Washington, D.C : Hemisphere Publishing Corporation.

Rohsenow, Warren M, Hartnett, James P and Cho, Young I. (1998), *Handbook of Heat Transfer*, New York; McGraw-Hill.

Win Aung, (1991) *Advances in Cooling Techniques for Computers*, Hemisphere Publishing Corporation.

Journals:

Alain Degiovanni, Benjamin Remy and Stephane Andre, (2003), " Thermal resistance of a multi –constrictions contact: A simple model", International Journal of Heat and Mass Transfer 46, 3727-3735.

Anthony F.Black, Vishal Singhal and Suresh V.Garimella (2004),"Analysis and Prediction of Constriction resistance for Contact Between rough Engineering Surfaces", Journal of Thermophysics and Heat Transfer, Vol.18, No.1, January-March 2004.

Chung, K.C Benson, H.K and Sheffeild, J.W,(1995),"Thermal Contact Conductance of Ceramic Substrate Junctions", Journal of Heat Transfer, May 1995, Vol.117.

ElSherbini, A.I, Jacobi, A.M and Hrnjak, P.S, (2003),"Experimental investigation of thermal contact resistance in plain-fin-tube evaporators with collarless fins", International Journal of Refrigeration 26 (2003) 527-536.

Greenwood, J.A and Tripp, J.H, (1970)" The Contact of Two Nominally Flat Rough Surfaces", Proc Instn Mech Engrs 1970-71 Vol 185 48/71.

Grujicic, M, Zhao, C.L, and Dusel, E.C, (2004), " The effect of thermal contact resistance on heat management in the electronic packaging", Applied Surface Science.

Gwinn, J. P. and Webb, R. L., "Performance and Testing of Thermal Interface Materials", (2003) Microelectronics Journal 34 (2003) 215-222

Juha Tuoriniemi, Kirsi Juntunen and Johanna Uusvuori,(2003),"Thermal contact to lithium metal", Physica B 329-333 (2003) 1294-1295.

Kikuo Kishimoto, Hirotsugu Inoue and Toshikazu Shibuya (1995), " Boundary element analysis of thermoelastic contact problems", Engineering Analysis with Boundary Elements 15 (1995) 329-337.

Knyazeva, A.G, (2000)," The conjugate problem of the thermal elasticity theory with imperfect heat contact between substances", Computational Materials Science 19 (2000) 252-260.

Koichi Nishino, Shigemasa Yamashita and Kahoru Torii, (1995), " Thermal Contact Conductance Under Low Applied load in a Vacuum Environment", Experimental Thermal and Fluid Science: 10.258-271.

Kutasov, I.M and Kagan, (2003)," Clindrical probe with a constant temperature-determination of the formation thermal conductivity and contact thermal resistance", Geothermics 32 (2003) 187-193.

Laraqi, N and Bairi, A, (2002)," Theory of thermal resistance between solids with randomly sized and located contacts", International Journal of Heat and Mass Transfer 45 (2002) 4175-4180.

Li, Y.Z, Madhusudana, C.V and Leonardi, E,(2000),"On the Enhancement of the Thermal Contact Conductance: Effect of Loading History", Journal of Heat Transfer, February 200, Vol.122.

Madhusudana, Chakravarti V, (1999),"Thermal conductance of cylindrical joints", International Journal of Heat and Mass Transfer 42 (1999) 1273-1287.

Madhusudana, C.V, (2000)," Accuracy In Thermal Contact Conductance-The Effect of Heat Losses to The Surroundings", Int. Comm. Heat Mass Transfer Vol.27, No.6,pp.877-891.

Marotta, E, Fletcher, L.S, Aikawa, T, Maki, K and Aoki, Y, (1999)," Thermal Contact Conductance of Sintered Copper Coatings on Ferro-Alloy", Journal of Heat Transfer, Febuary 1999, Vol.12.

Milanez, Fernando H, Yovanovich, M.M, and Culham, J.R, (2003), " Effect of Surface Asperity Truncation on Thermal Contact Conductance", IEEE Transactions on Components and Packaging Technologies, Vol.26, No.1,

Milanez, Fernando H, Yovanovich, Michael M, and Mantelli, Marcia B.H, (2004)," Thermal Contact Conductance at Low Contact Pressures", Journal of Thermophysics and Heat Transfer, Vol.18, No.1, January-March 2004.

Muzychka, Y.S, Sridhar,M.R and Yovanovich,M.M, (1999), " Thermal Spreading Resistance in Multilayered Contacts: Application in Thermal Contact Resistance", Journal of Thermophysics and Heat Transfer, Vol 13, No.4, October-December 1999.

Nakayama, Wataru and Bergles, Arthur E. (2003), " Thermal Interfacing Techniques for Electronic Equipment-A Perspetive", Journal of Electronic Packaging, Transaction of the ASME, Vol.125.

Neubauer, E, Korb, G, Eisenmenger-Sittner, C, Bangert, H, Chotikaprakhan, S, Deitzel, D, Mansanares, A.M and Bein, B.K, (2003),"The influence of mechanical adhesion of copper coatings on carbon surfaces on the interfacial thermal contact resistance", Thin Solid Films 433 (2003) 160-165.

Parihar, Shailendra K. and Wright, Neil T. (1997), " Thermal Contact Resistance at Elastomer to Metal Interfaces", Int. Comm. Heat Mass Transfer, Vol.24, No.8, pp.1083-1092.

Ponappan, Rengasamy and Ravigururajan, T.S, (2004) " Contact thermal resistance of Li-ion cell electrode stack", Journal of Power Sources 129 (2004) 7-13.

Salti, B and Laraqi, N, (1999)," 3-D numerical modeling of heat transfer between two sliding bodies; temperature and thermal contact resistance", International Journal of Heat and Mass Transfer 42 (1999) 2363-2374.

Song, S and Yovanovich, M.M, (1988), " Relative Contact Pressure: Dependence on Surface Roughness and Vickers Microhardness", J. Thermophysics, Vol.2, No.1, January 1988, American Institute of Aeronautics and Astronautics, Inc.

Trujillo, David M, and Pappoff, Chris G, (2002)," A General thermal contact resistance finite element", Finite Element in Analysis and Design 38 (2002) 263-276.

Wahid, Syed M. S. and Madhusudana, C. V., (2000) "Gap Conductance in Contact heat Transfer", International Journal of Heat and Mass Transfer, 43 (2000) 4483-4487 .

Wahid, Syed M. S. and Madhusudana, C. V, (2003)," Thermal contact conductance: effect of overloading and load cycling", International Journal of Heat and Mass Transfer 46 (2003) 4139-4143.

Wahid, S.M.S, Madhusudana, C.V, and Leonardi, E, (2004)," Solid spot conductance at low contact pressure", Experimental Thermal and Fluid Science 28 (2004) 489-494.

Wolf, E.G, and Schneider, D.A, (1998) "Prediction of Thermal Contact Resistance Between Polished Surfaces", International Journal of Heat and Mass Transfer, 41, 3469-3482.

Yeau-Ren Jeng, Jen-Tin Chen and Ching-Yang Cheng,(2005),"Thermal contact conductance of coated surfaces", Wear xxx (2005) xxx-xxx.

Yeh, C.L and Lin, C.T, (2003a), "Thermal Contact Resistance Correlation for Metals Across Bolted Joints", Int. Comm. Heat Mass Transfer, Vol.30, No.7, pp.987-996.

Yeh, C. L., Chen, Y. F., Wen, C. Y. and Li, K.T., (2003b) "Measurement of Thermal Contact Resistance of Aluminium Honeycombs", Experimental Thermal and Fluid Science, 27, 271 – 281.

Yovanovich, M.M., Culham, J. R. and Teertstra, P., "Calculating Interface Resistance" – Article 3 May, 1997, Microelectronics Heat Transfer Laboratory Department of Mechanical Engineering University of Waterloo.

Zhang, Zhe, Marotta, E.E, and Ochterbeck, J.M, (2003)," Thermal and Mechanical Model for Rigid Cylinder Indenting an Elastic Layer Resting on Rigid base: Application to Turned Surfaces", Journal of Electronic Packaging June 2003, Vol. 125, 186-191.

Proceedings:

Ismail, A.Kamal, Najhan, M.Awang and Abdullah, M.Z, (2004),"Experimental Investigation on Thermal Contact Resistance for Li-ion Cell Battery", Proceedings of the 6th International Conference On Electronic Materials and Packaging (EMAP), December 5-7, 2004.

Thesis:

Nazri & Abdullah (2001)

Web Site:

Gerald Recktenwald, (2004)," Thermal Contact Resistance in Electronic Cooling Applications", Lectures slide in ME 449/549 Thermal Management Laboratory, Portland State University, Department of Mechanical Engineering. [Online],[Accessed in March 2005]. Available from World Wide Web: www.me.pdx.edu/~gerry/class/ME449

Section 7, Step 4, Calculating the Combined Uncertainty,[online],[Accessed 6th June 2005). Available from World Wide Web:
http://www.measurementuncertainty.org/mu/guide/stepcalculating.html

Online Material Property.],[Accessed in 2005]. Available from World Wide Web www.matweb